CHAPTER 66

The DTFT and DFT

In Chapter 3 we showed that interesting waveforms can be synthesized by summing sinusoids or complex exponential signals having different frequencies and complex amplitudes as in the synthesis equation

$$x(t) = \sum_{k=-\infty}^{\infty} a_k e^{j2\pi f_0 k t}, \tag{66.1}$$

where $f_0 = 1/T_0$, and all the $\{a_k\}$ coefficients are known complex values. When the frequencies are integer multiples of a common fundamental frequency as in (66.1), the signal is periodic, and such a sum is called a *Fourier series* or a *Fourier synthesis equation*. We also introduced the concept of the *spectrum* of a signal as the collection of information about the frequencies and corresponding complex amplitudes, $\{kf_0, a_k\}$ of the sinusoidal or complex exponential signals in the Fourier series representation. We found it convenient to display the spectrum as a plot of amplitude and phase as a function of the discrete frequencies in the Fourier series. This spectrum plot tells us at a glance "how much of each frequency is present in the signal".

Given a mathematical Fourier series formula in the form (66.1), it is straightforward to plot the spectrum of the signal. The more challenging problem is to start from the signal $x(t)$ and determine its spectrum, but we showed that if we know the period T_0 and a formula for the time signal $x(t)$ as a function over one period (such as $0 \leq t \leq T_0$), then we can determine the value of each a_k coefficient in (66.1) by evaluating the integral

$$a_k = \frac{1}{T_0} \int_0^{T_0} x(t) e^{-j2\pi f_0 k t} dt. \tag{66.2}$$

By evaluating (66.2), we have *analyzed* the signal to determine its spectrum. This process is called *spectrum analysis* or, more specifically, *Fourier analysis*. In Chapter 3, we demonstrated Fourier analysis only for periodic continuous-time signals defined by an analytic formula, but the concept of (Fourier) spectrum analysis has much more breadth and depth. In this chapter, we will broaden and deepen our knowledge of spectrum analysis by discussing methods of Fourier analysis that apply to sampled signals that do not have to be periodic, and even to cases where we will not have a convenient mathematical formula for the signal samples.

It is safe to say that spectrum analysis is one of the most common operations used in the practice of signal processing. Sooner or later, most scientists and engineers will encounter a situation where a "sampled data signal" has been obtained from an A-to-D converter and must be analyzed to determine its spectral properties. Often, spectrum analysis is used to discover whether or not the signal contains strong periodic components. A listing of natural phenomena that are cyclic, or nearly so, would contain hundreds of entries. Common

examples include speech and music signals, as well as other natural observations such as tides and yearly sun spot cycles. In the case of sampled signals, the question of interest is how to derive the spectrum by doing numerical operations on a signal that is defined only by a finite set of numbers. This process of going from the sampled signal to its spectrum is called *discrete-time spectrum analysis.*

The central theme of this chapter is "Fourier" methods to perform spectrum analysis of discrete-time signals. The basis for beginning our discussion is the frequency response as defined and discussed in some detail in Chapter 6. We will show that the frequency response function is a special case of a more general concept called the discrete-time Fourier transform (or briefly, DTFT). We will show how the DTFT can be thought of as a generalization of the spectrum concept because it provides a frequency-domain representation of a wide range of both finite- and infinite-length sequences. Then we will see that the DTFT representation has many features that make it attractive for the analysis and design of LTI systems. After defining and exploring the properties of the DTFT, we will define a numerically computable Fourier transform called the discrete-Fourier transform (or DFT). We will see that the DFT gives a spectrum representation of a finite-length sequence, which can also be used as a representation of a periodic sequence formed by infinite repetition of the corresponding finite-length sequence. Finally, we will show how the DFT can be used to compute (very efficiently) a spectrum representation of any sampled signal. Thus, the DFT becomes the core of the spectrogram which provides a time-frequency spectrum analysis by doing DFTs of successive short sections of a very long signal.

66-1 DTFT: Discrete-Time Fourier Transform

The concept of frequency response discussed in Chapter 6 emerged from analysis showing that if an input to an LTI discrete-time system is of the form $x[n] = e^{j\hat{\omega}n}$, then the corresponding output is $y[n] = H(e^{j\hat{\omega}})e^{j\hat{\omega}n}$. This fact, coupled with the principle of superposition for LTI systems leads to the fundamental result that the frequency response function $H(e^{j\hat{\omega}})$ is all we need to know about the system in order to determine the output due to any linear (additive) combination of signals of the form $e^{j\hat{\omega}n}$ or $\cos(\hat{\omega}n + \theta)$. For discrete-time filters such as the causal FIR filters discussed in Chapter 6, the frequency response function is obtained from the summation formula

$$H(e^{j\hat{\omega}}) = \sum_{n=0}^{M} h[n]e^{-j\hat{\omega}n} \tag{66.3}$$

In a mathematical sense, the impulse response $h[n]$ is *transformed* into the frequency response by the operation of evaluating (66.3) for each value of $\hat{\omega}$ over the domain $-\pi < \hat{\omega} \leq \pi$. The operation of transformation replaces a function of a discrete-time index n (a sequence) by a periodic function of the continuous frequency variable $\hat{\omega}$. By this transformation, the time-domain representation $h[n]$ is replaced by the frequency-domain representation $H(e^{j\hat{\omega}})$. For this notion to be complete and useful, we need to know that the result of the transformation is unique, and we need the ability to go back from the frequency-domain representation to the time-domain representation. That is, we need an *inverse transform* that recovers the original $h[n]$ from $H(e^{j\hat{\omega}})$. In Chapter 6, we showed that the sequence can be reconstructed from a frequency response represented in terms of powers of $e^{-j\hat{\omega}}$ as in (66.3) by simply picking off the coefficients of the polynomial; i.e., $h[n]$ is the coefficient of $e^{-j\hat{\omega}n}$. While this process can be effective if M is small, there is a much more powerful approach to inverting the transformation that holds even for infinite-length sequences.

In this section, we will show that the frequency response is identical to the result of applying a more general concept called the *discrete-time Fourier transform* to the impulse response of the LTI system. We will derive an integral form for the inverse discrete-time Fourier transform that can be used even when $H(e^{j\hat{\omega}})$ does not have a finite polynomial representation such as (66.3). Furthermore, we will show that the discrete-time Fourier transform can be used to represent a wide range of sequences, including sequences of infinite length,

and that these sequences can be impulse responses, inputs to LTI systems, outputs of LTI systems, or indeed, any sequence that satisfies certain conditions to be discussed in this chapter.

66-1.1 The Discrete-Time Fourier Transform

The discrete-time Fourier transform or *DTFT*, is defined as

Discrete-Time Fourier Transform

$$X(e^{j\hat{\omega}}) = \sum_{n=-\infty}^{\infty} x[n]e^{-j\hat{\omega}n} \tag{66.4}$$

Note that for purposes of the definition, the DTFT is denoted $X(e^{j\hat{\omega}})$ and the corresponding sequence is $x[n]$. Going from the signal $x[n]$ to its DTFT is called "taking the forward transform"; from the DTFT back to the signal, "taking the inverse transform." The limits on the sum are infinite so that the DTFT will be defined for infinitely long signals as well as finite-length signals. However, a comparison of (66.4) to (66.3) shows that if the sequence were a finite-length impulse response, then the DTFT of that sequence would be the frequency response of the FIR system. More generally, if $h[n]$ is the impulse response of an LTI system, then the DTFT of $h[n]$ is the frequency response $H(e^{j\hat{\omega}})$ of that system. Examples of infinite-duration impulse response filters will be given in Chapter 8.

EXERCISE 66.1: Show that $X(e^{j\hat{\omega}})$ defined in (66.4) is always periodic in $\hat{\omega}$ with period 2π, i.e.,

$$X(e^{j(\hat{\omega}+2\pi)}) = X(e^{j\hat{\omega}}).$$

66-1.1.1 DTFT of a Shifted Impulse Sequence

Our first task is to develop examples for the DTFT for some common signals. The simplest case is the unit-impulse signal. Consider the sequence $x[n] = \delta[n - n_0]$. Its forward DTFT is by definition

$$X(e^{j\hat{\omega}}) = \sum_{n=-\infty}^{\infty} \delta[n - n_0]e^{-j\hat{\omega}n}$$

Since the impulse sequence is nonzero only at $n = n_0$ it follows that the sum has only one nonzero term, so

$$X(e^{j\hat{\omega}}) = e^{-j\hat{\omega}n_0}$$

To emphasize the importance of this and other DTFT relationships, we use the the notation $\overset{\text{DTFT}}{\rightleftarrows}$ to denote the forward and inverse transforms in one statement:

DTFT Representation of $\delta[n - n_0]$

$$x[n] = \delta[n - n_0] \overset{\text{DTFT}}{\rightleftarrows} X(e^{j\hat{\omega}}) = e^{-j\hat{\omega}n_0} \tag{66.5}$$

The DTFT is a *unique* relationship between $x[n]$ and $X(e^{j\hat{\omega}})$; in other words, two different signals cannot have the same DTFT. Because of this, if we know a DTFT representation such as (66.5), we can start in either the time or frequency domain and easily write down the corresponding representation in the other domain. For example, if $X(e^{j\hat{\omega}}) = e^{-j\hat{\omega}3}$ then we know that $x[n] = \delta[n - 3]$.

66-1.1.2 DTFT of a Pulse

Another common signal is the L-point pulse. Its DTFT is easy to obtain because it is the same as a known frequency response.

DTFT Representation of L-point pulse

$$x[n] = u[n] - n[n-L] \overset{\text{DTFT}}{\rightleftarrows} X(e^{j\hat{\omega}}) = \frac{\sin(L\hat{\omega}/2)}{\sin(\hat{\omega}/2)} e^{-j\hat{\omega}(L-1)/2} \tag{66.6}$$

The L-point pulse is a finite-length time signal consisting of all ones:

$$x[n] = u[n] - u[n-L] = \begin{cases} 1 & n = 0, 1, 2, \ldots, L-1 \\ 0 & \text{elsewhere} \end{cases}$$

Its forward DTFT is by definition

$$X(e^{j\hat{\omega}}) = \sum_{n=0}^{L-1} 1\, e^{-j\hat{\omega}n}$$

This is a signal whose frequency response is known, because the L-point pulse can be the impulse response of a running-sum FIR filter. In Sect. 6-7 the frequency response of the running-average filter was shown to be the product of a Dirichlet function and a complex exponential. The filter coefficients of the running-sum filter are L times the filter coefficients of the running-average filter, so there is no L in the denominator of (66.6).

66-1.1.3 DTFT of a Right-Sided Exponential Sequence

As an illustration of the DTFT of an infinite-duration sequence, consider a "right-sided" exponential[1] signal of the form $x[n] = a^n u[n]$. Such a signal is zero for $n < 0$ (on the lefthand side of a plot), and it will decay "exponentially" for $n \geq 0$ if $|a| < 1$, remain constant at 1 if $a = 1$, and grow exponentially if $|a| > 1$. Its DTFT is by definition

$$X(e^{j\hat{\omega}}) = \sum_{n=-\infty}^{\infty} a^n u[n] e^{-j\hat{\omega}n} = \sum_{n=0}^{\infty} a^n e^{-j\hat{\omega}n}$$

We can obtain a "closed form" expression for $X(e^{j\hat{\omega}})$ by noting that

$$X(e^{j\hat{\omega}}) = \sum_{n=0}^{\infty} (ae^{-j\hat{\omega}})^n,$$

which can now be recognized as the sum of all the terms of an infinite geometric series where the ratio between successive terms is $(ae^{-j\hat{\omega}})$. For such a series there is a formula for the sum that we can apply to give the final result

$$X(e^{j\hat{\omega}}) = \sum_{n=0}^{\infty} (ae^{-j\hat{\omega}})^n = \frac{1}{1 - ae^{-j\hat{\omega}}}$$

There is one limitation, however. Going from the infinite sum to the closed-form result is only valid when $|ae^{-j\hat{\omega}}| < 1$ or $|a| < 1$. Otherwise, the terms in the geometric series grow without bound and their sum will be infinite.

[1] An exponential signal would be written as $e^{\beta n}$, but since $e^{\beta n} = (e^{\beta})^n$ we use the more compact form a^n where $a = e^{\beta}$.

This DTFT is another very useful result, worthy of highlighting.

DTFT Representation of $a^n u[n]$

$$x[n] = a^n u[n] \overset{\text{DTFT}}{\rightleftarrows} X(e^{j\hat{\omega}}) = \frac{1}{1 - ae^{-j\hat{\omega}}} \quad \text{if } |a| < 1 \tag{66.7}$$

EXERCISE 66.2: Determine the signal whose DTFT is

$$X(e^{j\hat{\omega}}) = \frac{1}{1 - 0.5e^{-j\hat{\omega}}}$$

Use the uniqueness property of the DTFT along with (66.7) to find $x[n]$.

66-1.1.4 Existence of the DTFT

In the case of finite-length sequences such as the frequency response of an FIR filter in (66.3), the sum defining the DTFT is always finite for any $\hat{\omega}$; i.e., the frequency response of an FIR filter always exists (is finite). However, in the general case, where either the upper or lower or both of the limits on the sum in (66.4) are infinite, this may not be true. This is illustrated by the right-sided exponential sequence in Section 66-1.1.3.

A sufficient condition for the existence of the DTFT of a sequence $x[n]$ emerges from the following manipulation:

$$\begin{aligned}
|X(e^{j\hat{\omega}})| &= \left| \sum_{n=-\infty}^{\infty} x[n] e^{-j\hat{\omega}n} \right| \\
&\leq \sum_{n=-\infty}^{\infty} \left| x[n] e^{-j\hat{\omega}n} \right| \qquad (\textit{magnitude of sum} \leq \textit{sum of magnitudes}) \\
&\leq \sum_{n=-\infty}^{\infty} |x[n]| \underbrace{\left| e^{-j\hat{\omega}n} \right|}_{1} \qquad (\textit{magnitude of product} = \textit{product of magnitudes}) \\
&\leq \sum_{n=-\infty}^{\infty} |x[n]|
\end{aligned}$$

It follows that a sufficient condition for the existence of the DTFT of $x[n]$ is

Sufficient Condition for Existence of the DTFT

$$\left| X(e^{j\hat{\omega}}) \right| \leq \sum_{n=-\infty}^{\infty} |x[n]| < \infty \tag{66.8}$$

A sequence $x[n]$ satisfying (66.8) is said to be *absolutely summable*, and the infinite sum of the definition of $X(e^{j\hat{\omega}})$ in (66.4) is said to *converge* to a finite result for all $\hat{\omega}$.

Example 66-1: DTFT of Complex Exponential?

Consider a right-sided complex exponential sequence, $x[n] = e^{j\hat{\omega}_0 n}u[n]$. Applying the condition of (66.8) to this sequence leads to

$$\sum_{n=0}^{\infty} |e^{j\hat{\omega}_0 n}| = \sum_{n=0}^{\infty} 1 \rightarrow \infty$$

Thus, the DTFT of a complex exponential does not exist; the same is true for any infinite-duration sinusoid. On the other hand, if $|a| < 1$, the DTFT of $x[n] = a^n u[n]$ exists and is given by the result of Section 66-1.1.3. ■

66-1.2 The Inverse DTFT

Now that we have a condition for the existence of the DTFT, we need to address the question of the inverse discrete-time Fourier transform. It can be argued that if we have a table of known DTFT pairs such as (66.5) and (66.7), we can always go back and forth between the time-domain and frequency-domain representations simply by table lookup as in Exercise 66.2. However, with this approach, we would always be limited by the size of our table of known DTFT pairs.

Instead, we want to continue the development of the DTFT by determining an expression for the inverse discrete-time Fourier transform. We will see that the inverse transform provides us with a new set of powerful tools for the analysis of signals and systems. We will show that integral in equation (66.9) gives the inverse DTFT in terms of normalized frequency $\hat{\omega}$, and thus it is the desired partner to the DTFT equation (66.4).

Inverse DTFT

$$x[n] = \frac{1}{2\pi}\int_{-\pi}^{\pi} X(e^{j\hat{\omega}})e^{j\hat{\omega}n}\,d\hat{\omega}. \tag{66.9}$$

Observe that n is an integer variable in this equation, while $\hat{\omega}$ now is a dummy variable of integration that disappears when the definite integral is evaluated. The variable n can take on all integer values in the range $-\infty < n < \infty$, and hence, using (66.9) we can compute each sample of a sequence whose DTFT is $X(e^{j\hat{\omega}})$.

We can verify the validity of this expression by substituting $X(e^{j\hat{\omega}})$ in (66.4) into the righthand side of (66.9); i.e.,

$$\frac{1}{2\pi}\int_{-\pi}^{\pi} X(e^{j\hat{\omega}})e^{j\hat{\omega}n}\,d\hat{\omega} = \frac{1}{2\pi}\int_{-\pi}^{\pi}\left(\sum_{k=-\infty}^{\infty} x[k]e^{-j\hat{\omega}k}\right)e^{j\hat{\omega}n}\,d\hat{\omega} \tag{66.10}$$

where we have changed the index of summation to k to distinguish it from n. If the sequence $x[n]$ satisfies the condition of (66.8), then it is permissible to interchange the order of integration and summation leading to

$$\frac{1}{2\pi}\int_{-\pi}^{\pi} X(e^{j\hat{\omega}})e^{j\hat{\omega}n}\,d\hat{\omega} = \sum_{k=-\infty}^{\infty} x[k]\underbrace{\left(\frac{1}{2\pi}\int_{-\pi}^{\pi} e^{j\hat{\omega}(n-k)}\,d\hat{\omega}\right)}_{=\delta[n-k]} \tag{66.11}$$

Now consider the term in parentheses in (66.11). First note that when $k = n$,

$$\frac{1}{2\pi}\int_{-\pi}^{\pi} e^{j\hat{\omega}(n-k)}d\hat{\omega} = \frac{1}{2\pi}\int_{-\pi}^{\pi} d\hat{\omega} = 1 \qquad k = n \tag{66.12a}$$

and when $k \neq n$,

$$\frac{1}{2\pi}\int_{-\pi}^{\pi} e^{j\hat{\omega}(n-k)}d\hat{\omega} = \frac{1}{2\pi}\frac{e^{j\hat{\omega}(n-k)}}{j\hat{\omega}(n-k)}\bigg|_{-\pi}^{\pi} = \frac{e^{j\pi(n-k)} - e^{-j\pi(n-k)}}{j2\pi(\pi-(-\pi))(n-k)} = 0 \qquad k \neq n \tag{66.12b}$$

since the numerator is zero for any integers n and k, and the denominator is nonzero for $n \neq k$. Equations (66.12a) and (66.12b) show that the complex exponentials $e^{j\hat{\omega}n}$ and $e^{-j\hat{\omega}k}$ (when viewed as periodic functions of $\hat{\omega}$) are *orthogonal* to each other.[2] This basic property of complex exponentials can be applied to simplify (66.11) by noting that the term in parentheses simply selects the $k = n$ term in the infinite sum, and therefore,

$$\frac{1}{2\pi}\int_{-\pi}^{\pi} X(e^{j\hat{\omega}})e^{j\hat{\omega}n}d\hat{\omega} = x[n] \tag{66.13}$$

Thus, we have demonstrated that the sequence can be recovered from the DTFT by the integral operation of (66.9), and (66.9) is indeed the desired inverse transformation for the DTFT.

EXERCISE 66.3: Recall that $X(e^{j\hat{\omega}})$ defined in (66.4) is always periodic in $\hat{\omega}$ with period 2π. Use this fact and a change of variables to argue that we can rewrite the inverse DTFT integral with limits that go from 0 to 2π, instead of $-\pi$ to $+\pi$.

66-1.2.1 DTFT of a sinc Function

Consider the discrete-time signal

$$x[n] = \frac{\sin(\hat{\omega}_b n)}{\pi n} \qquad -\infty < n < \infty \tag{66.14}$$

where $0 < \hat{\omega}_b < \pi$. This mathematical form, which is called a "sinc" function, is plotted in Fig. 66-1(a) for $\hat{\omega}_b = 0.25\pi$. Although the sinc function appears to be undefined at $n = 0$, a careful application of L'Hôpital's rule, or the small angle approximation to the sine function, shows that the value is actually $x[0] = \hat{\omega}_b/\pi$. The sinc signal is important in discrete-time signal and system theory, but it is impossible to determine its DTFT by directly applying the forward transform summation (66.4). However, because of the uniqueness of the DTFT, we can obtain the desired DTFT transform pair if we can choose the correct transform $X(e^{j\hat{\omega}})$ and show that the inverse DTFT of $X(e^{j\hat{\omega}})$ determined by evaluation of (66.9) is the sinc function sequence.

As we will now show, the DTFT of the sinc function in (66.14) is an example of an *ideal band limited signal*; i.e., it is a function that is nonzero in the low frequency band $|\hat{\omega}| \leq \hat{\omega}_b$ (a constant value of one in this example) and zero in the high frequency band $\hat{\omega}_b < \hat{\omega} \leq \pi$, viz.,

$$X(e^{j\hat{\omega}}) = \begin{cases} 1 & |\hat{\omega}| \leq \hat{\omega}_b \\ 0 & \hat{\omega}_b < |\hat{\omega}| \leq \pi \end{cases}$$

[2] This same property was used in Section 3-4 to derive the Fourier series integral for periodic continuous-time signals. Note for example, the similarity between equations (3.21) and (66.9).

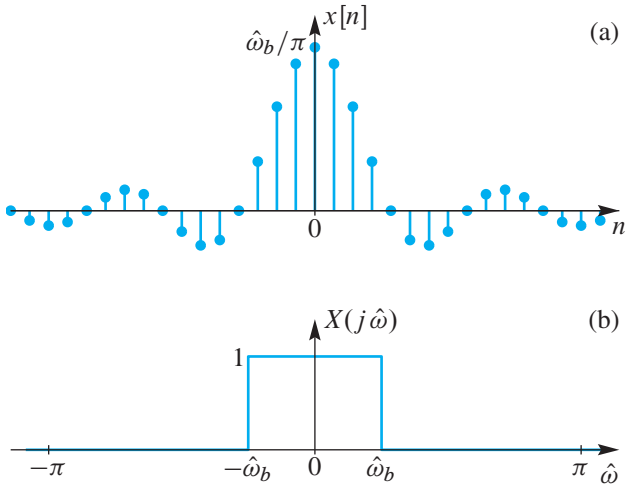

Figure 66-1: (a) Sinc function for $\hat{\omega}_b = 0.25\pi$. (b) Corresponding DTFT.

The DTFT of the sinc function is plotted in Fig. 66-1(b). This piecewise constant function is relatively easy to integrate after we plug the definition of $X(e^{j\hat{\omega}})$ into the inverse DTFT integral (66.9)

$$x[n] = \frac{1}{2\pi}\int_{-\pi}^{\pi} X(e^{j\hat{\omega}})e^{j\hat{\omega}n}\,d\hat{\omega} = \frac{1}{2\pi}\int_{-\pi}^{-\hat{\omega}_b} 0\,e^{j\hat{\omega}n}\,d\hat{\omega} + \frac{1}{2\pi}\int_{-\hat{\omega}_b}^{\hat{\omega}_b} 1\,e^{j\hat{\omega}n}\,d\hat{\omega} + \frac{1}{2\pi}\int_{\hat{\omega}_b}^{\pi} 0\,e^{j\hat{\omega}n}\,d\hat{\omega}$$

Only the middle integral is nonzero, and the integration yields

$$\begin{aligned} x[n] &= \frac{1}{2\pi}\int_{-\hat{\omega}_b}^{\hat{\omega}_b} 1\,e^{j\hat{\omega}n}\,d\hat{\omega} \\ &= \frac{e^{j\hat{\omega}n}}{2\pi jn}\bigg|_{-\hat{\omega}_b}^{\hat{\omega}_b} = \frac{e^{j\hat{\omega}_b n} - e^{-j\hat{\omega}_b n}}{(2j)\pi n} = \frac{\sin(\hat{\omega}_b n)}{\pi n} \end{aligned}$$

The last step uses the inverse Euler formula for sine. Since a DTFT pair is unique, we have proven that the forward DTFT of a sinc function is a rectangle in the frequency domain:

$$X(e^{j\hat{\omega}}) = \sum_{n=-\infty}^{\infty} \frac{\sin(\hat{\omega}_b n)}{\pi n} e^{-j\hat{\omega}n} = \begin{cases} 1 & |\hat{\omega}| \le \hat{\omega}_b \\ 0 & \text{otherwise} \end{cases}$$

Thus, we have obtained another DTFT pair that can be added to our growing inventory.

DTFT Representation of a Sinc Function

$$x[n] = \frac{\sin(\hat{\omega}_b n)}{\pi n} \overset{\text{DTFT}}{\rightleftarrows} X(e^{j\hat{\omega}}) = \begin{cases} 1 & |\hat{\omega}| \le \hat{\omega}_b \\ 0 & \text{otherwise} \end{cases} \tag{66.15}$$

66-1.2.2 Inverse DTFT for the Right-Sided Exponential

Another infinite-length sequence is the right-sided exponential signal $x[n] = a^n u[n]$ discussed in Section 66-1.1.3. In this case, we were able to use a familiar result for geometric series to "sum" the expression for the DTFT and obtain a closed-form representation

$$X(e^{j\hat{\omega}}) = \frac{1}{1 - ae^{-j\hat{\omega}}} \qquad |a| < 1 \tag{66.16}$$

On the other hand, suppose that we want to determine $x[n]$ given $X(e^{j\hat{\omega}})$ in (66.16). Substituting this into the inverse DTFT expression (66.9) gives

$$x[n] = \frac{1}{2\pi} \int_{-\pi}^{\pi} \frac{e^{j\hat{\omega}n}}{1 - ae^{-j\hat{\omega}}} d\hat{\omega} \tag{66.17}$$

Although techniques exist for evaluating such integrals using the theory of complex variables, we do not assume knowledge of these techniques, and showing that (66.17) evaluates to $x[n] = a^n u[n]$ would be a difficult and tedious exercise in integral calculus. However, all is not lost. We can always rely on the tabulated result in (66.7), and we can write the inverse transform by inspection.

The examples in Sections 66-1.2.1 and 66-1.2.2 illustrate an important point about the DTFT representation. For the sinc function example in Section 66-1.2.1, it was relatively easy to go from the frequency-domain representation to the time-domain representation, but impossible to go the other direction. On the other hand, for the exponential sequence in Section 66-1.2.2, the opposite was true. The important point of both examples is that once a transform pair has been determined, by what ever means, we can use that DTFT relationship to move back and forth between the time and frequency domains with little effort. In Section 66-2 we will show that a number of general properties of the DTFT can be employed to simplify discrete-time Fourier analysis even more.

66-1.3 The DTFT is the Spectrum

So far, we have not used the term "spectrum" when discussing the DTFT, but it should be clear at this point that it is appropriate to refer to the DTFT as a spectrum representation of a discrete-time signal. Recall that we introduced the term spectrum in Chapter 3 to mean the collection of frequency and complex amplitude information required to synthesize a signal using the Fourier synthesis equation in (66.1). In the case of the DTFT, the synthesis equation is the inverse transform integral (66.9), and the analysis equation (66.4) provides a means for determining the complex amplitudes of the complex exponentials $e^{j\hat{\omega}n}$ in the synthesis equation. To make this a little more concrete, we can view the inverse DTFT integral as the limit of a finite sum by writing (66.9) in terms of the Riemann sum definition[3] of the integral

$$x[n] = \frac{1}{2\pi} \int_{0}^{2\pi} X(e^{j\hat{\omega}}) e^{j\hat{\omega}n} d\hat{\omega} = \lim_{\Delta\hat{\omega}\to 0} \sum_{k=0}^{N-1} \left(\frac{1}{2\pi} X(e^{j\hat{\omega}_k}) \Delta\hat{\omega} \right) e^{j\hat{\omega}_k n} \tag{66.18}$$

where $\Delta\hat{\omega} = 2\pi/N$ is the spacing between the frequencies $\hat{\omega}_k = 2\pi k/N$, with the range of integration[4] $0 \le \hat{\omega} < 2\pi$ being covered by choosing $k = 0, 1, \ldots, N-1$. The expression on the right in (66.18) contains a

[3] The Riemann-sum approximation to an integral is $\int_0^u q(t)dt \approx \sum_{n=0}^{N_u-1} q(t_n)\Delta t$, where the integrand $q(t)$ is sampled at N_u equally spaced times $t_n = n\Delta t$, and $\Delta t = u/N_u$.

[4] We have used the result of Exercise 66.3 to change the limits to 0 to 2π.

sum of complex exponential signals whose spectrum representation is the set of frequencies $\hat{\omega}_k$ together with the corresponding complex amplitudes $X(e^{j\hat{\omega}_k})\Delta\hat{\omega}/(2\pi)$. This is illustrated in Fig. 66-2 which shows the values $X(e^{j\hat{\omega}_k})$ as gray dots and the rectangles have area equal to $X(e^{j\hat{\omega}_k})\Delta\hat{\omega}$. Each one of the rectangles can be viewed as a spectrum line, especially when $\Delta\hat{\omega} \to 0$. In the limit as $\Delta\hat{\omega} \to 0$, the magnitudes of

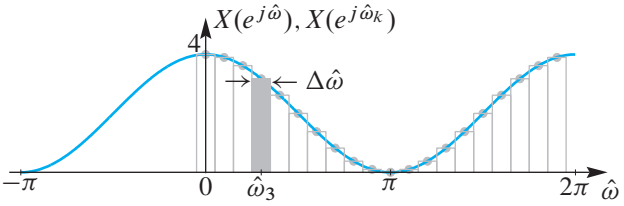

Figure 66-2: Riemann sum approximation to the integral of the inverse DTFT. Here, $X(e^{j\hat{\omega}}) = 2(1 + \cos\hat{\omega})$ which is the DTFT of $x[n] = \delta[n+1] + 2\delta[n] + \delta[n-1]$.

the spectral components become infinitesimally small, as does the spacing between frequencies. Therefore, (66.18) suggests that the inverse DTFT integral synthesizes the signal $x[n]$ as a sum of infinitely small complex exponentials with all frequencies $0 \le \hat{\omega} < 2\pi$ being used in the sum. The changing magnitude of $X(e^{j\hat{\omega}})$ specifies the relative amount of each frequency component that is required to synthesize $x[n]$. This is entirely consistent with the way we originally defined and subsequently used the concept of spectrum in Ch. 3, so we will apply the term *spectrum* also to the DTFT representation.

66-2 Properties of the DTFT

We have motivated our study of the DTFT primarily by considering the problem of determining the frequency response of a filter, or more generally the Fourier representation of a signal. While these are important applications of the DTFT, it is also important to note that the DTFT also plays an important role as an "operator" in the theory of discrete-time signals and systems. This is best illustrated by highlighting some of the important properties of the DTFT operator.

66-2.1 The Linearity Property

The DTFT of a sum of two or more sequences is equal to the sum of the corresponding DTFTs, and multiplying a sequence by a constant will scale its DTFT by the same constant. More formally, we can summarize this property by considering a sequence $x[n] = ax_1[n] + bx_2[n]$, where a and b are constants, and $x_1[n]$ and $x_2[n]$ are sequences having DTFTs $X_1(e^{j\hat{\omega}})$ and $X_2(e^{j\hat{\omega}})$, repectively. The DTFT operation obeys the scaling property and the principle of superposition; i.e., it is a linear operation. This is summarized in (66.19)

Linearity Property of the DTFT

$$x[n] = ax_1[n] + bx_2[n] \overset{\text{DTFT}}{\rightleftarrows} X(e^{j\hat{\omega}}) = aX_1(e^{j\hat{\omega}}) + bX_2(e^{j\hat{\omega}}) \tag{66.19}$$

66-2.2 The Time-Delay Property

When we first studied sinusoids, the phase was shown to depend on the time-shift of the signal. The simple relationship was "phase equals the negative of frequency times time-shift." This concept carries over to the

general case of the Fourier transform. The time-delay property of the DTFT states that time-shifting results in a phase change in the frequency domain:

Time-Delay Property of the DTFT

$$y[n] = x[n - n_d] \overset{\text{DTFT}}{\rightleftarrows} Y(e^{j\hat{\omega}}) = X(e^{j\hat{\omega}})e^{-j\hat{\omega}n_d} \tag{66.20}$$

The reason that the delay property is so important and useful is that equation (66.20) shows that multiplicative factors of the form $e^{-j\hat{\omega}n_d}$ in frequency-domain expressions always signify time delay.

Example 66-2: Delayed Sinc Function

Let $y[n] = x[n - 10]$ where $x[n]$ is the sinc function of (66.15); i.e.,

$$y[n] = \frac{\sin \hat{\omega}_b(n - 10)}{\pi(n - 10)}.$$

Using the time-delay property and the result for $X(e^{j\hat{\omega}})$ in (66.15), we can write down the following expression for the DTFT of $y[n]$ with virtually no further analysis:

$$Y(e^{j\hat{\omega}}) = X(e^{j\hat{\omega}})e^{-j\hat{\omega}10} = \begin{cases} e^{-j\hat{\omega}10} & 0 \le |\hat{\omega}| \le \hat{\omega}_b \\ 0 & \hat{\omega}_b < |\hat{\omega}| \le \pi \end{cases}$$

Notice that the magnitude plot of $|Y(e^{j\hat{\omega}})|$ is still a rectangle; only the phase changed. ■

To prove the time-delay property, consider a sequence $y[n] = x[n - n_d]$, which we see is simply a time-shifted version of another sequence $x[n]$. We need to compare the DTFT of $y[n]$ vis-à-vis the DTFT of $x[n]$. By definition, the DTFT of $y[n]$ is

$$Y(e^{j\hat{\omega}}) = \sum_{n=-\infty}^{\infty} \underbrace{x[n - n_d]}_{y[n]} e^{-j\hat{\omega}n}. \tag{66.21}$$

If we make the substitution $m = n - n_d$ for the index of summation in (66.21), we obtain

$$Y(e^{j\hat{\omega}}) = \sum_{m=-\infty}^{\infty} x[m]e^{-j\hat{\omega}(m+n_d)} = \sum_{n=-\infty}^{\infty} x[m]e^{-j\hat{\omega}m}e^{-j\hat{\omega}n_d}. \tag{66.22}$$

Since the factor $e^{-j\hat{\omega}n_d}$ does not depend on m and is common to all the terms in the sum on the right in (66.22), we can write $Y(e^{j\hat{\omega}})$ as

$$Y(e^{j\hat{\omega}}) = \left(\sum_{n=-\infty}^{\infty} x[m]e^{-j\hat{\omega}m} \right) e^{-j\hat{\omega}n_d} = X(e^{j\hat{\omega}})e^{-j\hat{\omega}n_d}. \tag{66.23}$$

Therefore, we have proved that time-shifting results in a phase change in the frequency domain.

66-2.3 The Frequency-Shift Property

Consider a sequence $y[n] = e^{j\hat{\omega}_c n}x[n]$, whose DTFT turns out to be a frequency-shifted version of the DTFT of the sequence $x[n]$. The multiplication by a complex exponential causes the frequency shift in the DTFT of $y[n]$ vis-à-vis the DTFT of $x[n]$. By definition, the DTFT of $y[n]$ is

$$Y(e^{j\hat{\omega}}) = \sum_{n=-\infty}^{\infty} \underbrace{e^{j\hat{\omega}_c n}x[n]}_{y[n]} e^{-j\hat{\omega}n}. \tag{66.24}$$

If we combine the exponentials in summation on the right side of (66.24), we obtain

$$Y(e^{j\hat{\omega}}) = \sum_{n=-\infty}^{\infty} x[n]e^{-j(\hat{\omega}-\hat{\omega}_c)n} = X(e^{j(\hat{\omega}-\hat{\omega}_c)}) \tag{66.25}$$

Therefore, we have proved the following general property of the DTFT:

Frequency-Shift Property of the DTFT

$$y[n] = e^{j\hat{\omega}_c n}x[n] \overset{\text{DTFT}}{\rightleftarrows} Y(e^{j\hat{\omega}}) = X(e^{j(\hat{\omega}-\hat{\omega}_c)}) \tag{66.26}$$

Example 66-3: Exponentially Decaying Cosine Signal

A very common signal for modeling the response of physical systems is an oscillating signal whose amplitude is dropping. The precise form is an exponential times a sinusoid, $x[n] = a^n \cos(\hat{\omega}_0 n)u[n]$, which we can express as

$$x[n] = \tfrac{1}{2}e^{j\hat{\omega}_0 n}a^n u[n] + \tfrac{1}{2}e^{-j\hat{\omega}_0 n}a^n u[n]$$

Thus we have $a^n u[n]$ multiplied by two different complex exponential signals. Using the DTFT pair in (66.7) and applying the frequency-shift property (66.26) twice, we can write

$$X(e^{j\hat{\omega}}) = \frac{\frac{1}{2}}{1 - ae^{-j(\hat{\omega}-\hat{\omega}_0)}} + \frac{\frac{1}{2}}{1 - ae^{-j(\hat{\omega}+\hat{\omega}_0)}}$$

Finding a common denominator for the two fractions allows us to write the DTFT in the following form:

$$X(e^{j\hat{\omega}}) = \frac{1 - a\cos(\hat{\omega}_0)e^{-j\hat{\omega}}}{(1 - ae^{j\hat{\omega}_0}e^{-j\hat{\omega}})(1 - ae^{-j\hat{\omega}_0}e^{-j\hat{\omega}})} = \frac{1 - a\cos(\hat{\omega}_0)e^{-j\hat{\omega}}}{1 - 2a\cos(\hat{\omega}_0)e^{-j\hat{\omega}} + a^2e^{-j\hat{\omega}2}}$$

■

66-2.4 Convolution and the DTFT

Perhaps the most important property of the DTFT concerns the DTFT of a sequence that is the discrete-time convolution of two sequences. The following property says that the DTFT *transforms convolution into multiplication.*

Convolution Property of the DTFT

$$y[n] = x[n] * h[n] \overset{\text{DTFT}}{\rightleftarrows} Y(e^{j\hat{\omega}}) = X(e^{j\hat{\omega}})H(e^{j\hat{\omega}}) \tag{66.27}$$

For example, suppose that $y[n] = x[n] * h[n]$, where $y[n]$ is the output, $x[n]$ is the input, and $h[n]$ is the impulse response of an LTI discrete-time system. In Chapter 5, we studied convolution with a finite-length impulse response, but in the general case, the signals can all be infinitely long. Then $y[n]$ is formed by evaluating the convolution sum equation with infinite limits

$$y[n] = \sum_{m=-\infty}^{\infty} x[m]h[n-m] \qquad -\infty < n < \infty \tag{66.28}$$

The DTFT of $y[n]$ can, therefore, be expressed in the following equivalent forms:

$$\begin{aligned} Y(e^{j\hat{\omega}}) &= \sum_{n=-\infty}^{\infty} y[n]e^{-j\hat{\omega}n} && (66.29a)\\ &= \sum_{n=-\infty}^{\infty} \left(\sum_{m=-\infty}^{\infty} x[m]h[n-m] \right) e^{-j\hat{\omega}n} && (66.29b)\\ &= \sum_{m=-\infty}^{\infty} x[m] \left(\sum_{n=-\infty}^{\infty} h[n-m]e^{-j\hat{\omega}n} \right) && (66.29c) \end{aligned}$$

The third form, (66.29c), is obtained by interchanging the order of summations on n and m. Now, using the delay property of (66.20), the term inside the parentheses in (66.29c) is recognized as the DTFT of $h[n]$ shifted by m. Therefore, we can now write $Y(e^{j\hat{\omega}})$ as

$$\begin{aligned} Y(e^{j\hat{\omega}}) &= \sum_{m=-\infty}^{\infty} x[m] \left(e^{-j\hat{\omega}m} H(e^{j\hat{\omega}}) \right), && (66.29d)\\ &= \left(\sum_{m=-\infty}^{\infty} x[m]e^{-j\hat{\omega}m} \right) H(e^{j\hat{\omega}}), && (66.29e) \end{aligned}$$

where $H(e^{j\hat{\omega}})$ can be factored out in (66.29e) because it is common to all the terms in the sum. Recognizing that the term in the parentheses in (66.29e) is $X(e^{j\hat{\omega}})$, we obtain finally,

$$Y(e^{j\hat{\omega}}) = H(e^{j\hat{\omega}})X(e^{j\hat{\omega}}). \tag{66.30}$$

Thus, we see that convolution in the time-index domain has been transformed into multiplication in the DTFT frequency domain.

As we discussed in Section 66-1.3, the DTFT $X(e^{j\hat{\omega}})$ plays the role of spectrum for both finite-length signals and infinite-length signals The convolution property (66.27) reinforces this view. If we use (66.27) to write the expression for the output of an LTI system using the DTFT synthesis integral, we have

$$y[n] = \frac{1}{2\pi} \int_0^{2\pi} X(e^{j\hat{\omega}})H(e^{j\hat{\omega}})e^{j\hat{\omega}n}\,d\hat{\omega} = \lim_{\Delta\hat{\omega}\to 0} \sum_{k=0}^{N-1} \left(\frac{\Delta\hat{\omega}}{2\pi} X(e^{j\hat{\omega}_k})H(e^{j\hat{\omega}_k}) \right) e^{j\hat{\omega}_k n} \tag{66.31}$$

Now we see that the complex amplitude $\frac{\Delta\hat{\omega}}{2\pi}X(e^{j\hat{\omega}_k})$ at each frequency is modified by the frequency response $H(e^{j\hat{\omega}_k})$ of the system evaluated at the given frequency $\hat{\omega}_k$. This is exactly the same result as the *sinusoid-in gives sinusoid-out* property that we saw in Ch. 6 for case where the input is a discrete sum of complex exponentials.

Example 66-4: Frequency Response of Delay

The delay property is a special case of the convolution property of the DTFT. To see this, recall that we can represent delay as the convolution with a shifted impulse

$$y[n] = x[n] * \delta[n - n_d] = x[n - n_d],$$

so the impulse response of a delay system is $h[n] = \delta[n - n_d]$. The corresponding frequency response of the delay system is

$$H(e^{j\hat{\omega}}) = \sum_{n=-\infty}^{\infty} \delta[n - n_d]e^{-j\hat{\omega}n} = e^{-j\hat{\omega}n_d}$$

Therefore, using the convolution property, the DTFT of the output of the delay system is

$$Y(e^{j\hat{\omega}}) = X(e^{j\hat{\omega}})H(e^{j\hat{\omega}}) = X(e^{j\hat{\omega}})e^{-j\hat{\omega}n_d}$$

which is identical to the delay property of (66.20). ■

The convolution property of LTI systems provides an effective way to think about LTI systems. In particular, when we think of LTI systems as "filters" we are thinking of their frequency responses, which can be chosen so that some frequencies of the input are blocked while others pass through with little modification. In the next section, we will define several ideal frequency-selective filters whose frequency responses are ideal versions of filters that we might want to implement in a signal processing application.

66-2.5 Autocorrelation and Energy Spectrum

An important result in Fourier transforms is *Parseval's Theorem*:

Parseval's Theorem for the Energy of a Signal

$$\sum_{n=-\infty}^{\infty} |x[n]|^2 = \frac{1}{2\pi}\int_{-\pi}^{\pi} |X(e^{j\hat{\omega}})|^2 d\hat{\omega} \tag{66.32}$$

The lefthand side of (66.32) is called the energy in the signal; it is a scalar. Thus the righthand side of (66.32) is also the energy, but the DTFT $|X(e^{j\hat{\omega}})|^2$ shows how the energy is distributed versus frequency. Therefore, the DTFT $|X(e^{j\hat{\omega}})|^2$ is called the *magnitude-squared spectrum* or the *energy spectrum* of $x[n]$.[5] If we first define the energy of a signal as the sum of the squares

$$E = \sum_{n=-\infty}^{\infty} |x[n]|^2 \tag{66.33}$$

[5] In many physical system, energy is calculated by taking the square of a physical quantity (like voltage) and integrating, or summing, over time.

then the energy E is a single number that is often a convenient measure of the size of the signal.

Example 66-5: Energy of the Sinc Signal

The energy of the sinc signal (evaluated in the time domain) is

$$E = \sum_{n=-\infty}^{\infty} \left(\frac{\sin \hat{\omega}_b n}{\pi n} \right)^2$$

While it is impossible to evaluate this sum directly, application of Parseval's theorem yields

$$E = \sum_{n=-\infty}^{\infty} \left(\frac{\sin \hat{\omega}_b n}{\pi n} \right)^2 = \frac{1}{2\pi} \int_{-\hat{\omega}_b}^{\hat{\omega}_b} |1|^2 d\hat{\omega} = \frac{\hat{\omega}_b}{\pi}$$

because the DTFT of the sinc signal is one for $-\hat{\omega}_b \leq \hat{\omega} \leq \hat{\omega}_b$. A simple interpretation of this result is that the energy is proportional to the bandwidth of the sinc signal. ■

66-2.5.1 Autocorrelation Function

The energy spectrum is the Fourier transform of a time-domain signal which turns out to be the autocorrelation of $x[n]$. The autocorrelation function is widely used in signal detection applications. It can be defined in terms of the convolution operation as follows:

$$c_{xx}[n] = x[-n] * x[n] = \sum_{k=-\infty}^{\infty} x[-k]x[n-k] \tag{66.34}$$

EXERCISE 66.4: In (66.34) we use the time-reversed signal $x[-n]$. Show that the DTFT of $x[-n]$ is $X(e^{-j\hat{\omega}})$. Furthermore, show that when $x[n]$ is real, $X(e^{-j\hat{\omega}}) = X^*(e^{j\hat{\omega}})$.

By making the substitution $m = -k$ for the dummy index of summation, we can write

$$c_{xx}[n] = \sum_{k=-\infty}^{\infty} x[m]x[n+m] \qquad -\infty < n < \infty \tag{66.35}$$

which is the basic definition of the autocorrelation function for $x[n]$. Observe that in (66.35), the index n serves to shift $x[n+m]$ with respect to $x[m]$ when both sequences are thought of as functions of m. It can be shown that $c_{xx}[n]$ is maximum at $n = 0$; i.e., when $x[n+m]$ is perfectly aligned with $x[m]$. The independent variable n in $c_{xx}[n]$ is often called the "lag" by virtue of its meaning as a shift between two copies of the same sequence $x[n]$. From (66.35) it follows that $E = c_{xx}[0]$; i.e., the energy of a signal is the value of its autocorrelation function at $n = 0$.

EXERCISE 66.5: Determine and plot the autocorrelation function for the signal $x[n] = a^n u[n]$.

Using the results of Exercise 66.4for real signals, the DTFT of the autocorrelation function $c_{xx}[n] = x[-n] * x[n]$ is

$$C_{xx}(e^{j\hat{\omega}}) = X(e^{-j\hat{\omega}})X(e^{j\hat{\omega}}) = X^*(e^{j\hat{\omega}})X(e^{j\hat{\omega}}) = |X(e^{j\hat{\omega}})|^2 \tag{66.36}$$

A useful relationship results if we represent $c_{xx}[n]$ in terms of its inverse DTFT; i.e.,

$$c_{xx}[n] = \frac{1}{2\pi}\int_{-\pi}^{\pi} |X(e^{j\hat{\omega}})|^2 e^{j\hat{\omega}n}\, d\hat{\omega} \tag{66.37}$$

Once we evaluate both sides of (66.37) at $n = 0$, we see that the energy of the sequence can also be computed from $C_{xx}(e^{j\hat{\omega}}) = |X(e^{j\hat{\omega}})|^2$ as follows:

$$E = c_{xx}[0] = \frac{1}{2\pi}\int_{-\pi}^{\pi} |X(e^{j\hat{\omega}})|^2 d\hat{\omega} \tag{66.38}$$

Finally, equating (66.33) and (66.38) we obtain *Parseval's Theorem* (66.32).

66-3 Ideal Filters

In any practical application of LTI discrete-time systems, the frequency response function $H(e^{j\hat{\omega}})$ would be derived by a filter design procedure that would yield an LTI system that could be implemented with finite computation. However, in the early phases of the design of a system it is often useful to use *ideal filters* that have simple frequency responses that provide ideal frequency-selectivity.

66-3.1 Ideal Lowpass Filter

An ideal lowpass filter (LPF) has a frequency response that consists of two regions: the passband near $\hat{\omega} = 0$ (DC) where the frequency response is one, and the stopband, where it is zero. An ideal lowpass filter is therefore

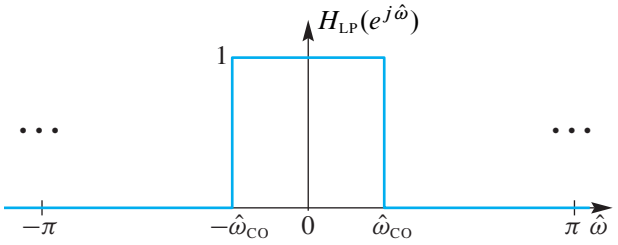

Figure 66-3: Frequency response of an ideal LPF with its cutoff at $\hat{\omega}_{CO}$ rad/s. Recall that $H_{LP}(e^{j\hat{\omega}})$ must also be periodic with period 2π.

defined as

$$H_{LP}(e^{j\hat{\omega}}) = \begin{cases} 1 & |\hat{\omega}| \le \hat{\omega}_{CO} \\ 0 & \hat{\omega}_{CO} < |\hat{\omega}| \le \pi \end{cases} \tag{66.39}$$

The frequency $\hat{\omega}_{CO}$ is called the *cutoff frequency*, or the band edge, of the LPF passband. Figure 66-3 shows a plot of $H_{LP}(e^{j\hat{\omega}})$ for the ideal LPF. The shape is rectangular and $H_{LP}(e^{j\hat{\omega}})$ is even symmetric about $\omega = 0$. As discussed in Section 6-4.3, this property is needed because real-valued impulse responses lead to filters

with a conjugate symmetric frequency responses. Since $H_{\rm LP}(e^{j\hat{\omega}})$ has zero phase, it is both real and conjugate symmetric, so it must be an even function.

EXERCISE 66.6: In Ch. 6 we saw that the frequency response for a real impulse response must be conjugate symmetric. Since the frequency response function is a DTFT, it must also be true that for every real $x[n]$, the corresponding DTFT is conjugate symmetric. Show that if $x[n]$ is real,

$$X(e^{-j\hat{\omega}}) = X^*(e^{j\hat{\omega}})$$

The impulse response of the ideal lowpass filter, found by applying the DTFT pair in (66.15), is the sinc function

$$h_{\rm LP}[n] = \frac{\sin \hat{\omega}_{\rm CO} n}{\pi n} \qquad -\infty < n < \infty \tag{66.40}$$

The ideal lowpass filter is impossible to implement because the impulse response $h_{\rm LP}[n]$ is non-causal and, in fact, nonzero over the entire time axis. However, that does not invalidate the ideal lowpass filter concept; i.e., the idea of selecting the low frequency band and rejecting all other frequencies. Even the moving average filter discussed in Section 6-7 might be a satisfactory lowpass filter in some applications. Figure 6-8 shows the frequency response of an 11-point moving averaged. Note that this causal filter has a low-pass-like frequency response magnitude, but it is far away from zero in what might be considered the stopband. In more stringent filtering applications, we need better approximations to the ideal characteristic. In a practical application, the process of filter design involves mathematical approximation of the ideal filter with a frequency response that is close enough to the ideal frequency response while corresponding to an implementable filter.

The following example shows the power of the transform approach when dealing with filtering problems.

Example 66-6: Ideal Lowpass Filtering

Consider an ideal lowpass filter with frequency response given by (66.39) and impulse response in (66.40). Now suppose that the input signal $x[n]$ to the ideal lowpass filter is a bandlimited sinc signal

$$x[n] = \frac{\sin \hat{\omega}_b n}{\pi n} \tag{66.41}$$

Working in the time domain, the corresponding output of the ideal lowpass filter would be given by the convolution expression

$$y[n] = x[n] * h_{\rm LP}[n] = \sum_{m=-\infty}^{\infty} \left(\frac{\sin \hat{\omega}_b m}{\pi m}\right)\left(\frac{\sin \hat{\omega}_{\rm CO}(n-m)}{\pi(n-m)}\right) \qquad -\infty < n < \infty \tag{66.42}$$

Evaluating this convolution directly in the time domain would be impossible both analytically and computationally. However, it is straightforward to obtain the filter output if we use the DTFT because in the frequency-domain the transforms are rectangles and they are multiplied. From (66.15), the DTFT of the input is

$$X(e^{j\hat{\omega}}) = \begin{cases} 1 & |\hat{\omega}| \le \hat{\omega}_b \\ 0 & \hat{\omega}_b < |\hat{\omega}| \le \pi \end{cases} \tag{66.43}$$

Therefore, the DTFT of the output of the filter is $Y(e^{j\hat{\omega}}) = X(e^{j\hat{\omega}})H(e^{j\hat{\omega}})$, which would be of the form

$$Y(e^{j\hat{\omega}}) = X(e^{j\hat{\omega}})H_{\text{LP}}(e^{j\hat{\omega}}) = \begin{cases} 1 & |\hat{\omega}| \leq \hat{\omega}_a \\ 0 & \hat{\omega}_a < |\hat{\omega}| \leq \pi \end{cases} \tag{66.44a}$$

where the cutoff frequency $\hat{\omega}_a$ is the smaller of $\hat{\omega}_b$ and $\hat{\omega}_{\text{CO}}$,

$$\hat{\omega}_a = \min(\hat{\omega}_b, \hat{\omega}_{\text{CO}}) \tag{66.44b}$$

In other words, the product of the two rectangles is another rectangle equal to the smaller of the two. Since we want to determine the output signal $y[n]$, we must take the inverse DTFT of $Y(e^{j\hat{\omega}})$. Thus, using (66.15) to do the inverse transformation, the convolution in (66.42) evaluates to another sinc function

$$y[n] = \sum_{m=-\infty}^{\infty} \left(\frac{\sin \hat{\omega}_b m}{\pi m}\right)\left(\frac{\sin \hat{\omega}_c (n-m)}{\pi (n-m)}\right) = \frac{\sin \hat{\omega}_a n}{\pi n} \qquad -\infty < n < \infty \tag{66.45}$$

where $\hat{\omega}_a = \min(\hat{\omega}_b, \hat{\omega}_c)$. ■

EXERCISE 66.7: The result given (66.44a) and (66.44b) is easily seen from a graphical solution that shows the rectangular shapes of the DTFTs. Sketch plots of $X(e^{j\hat{\omega}})$ from (66.43) and $H_{\text{LP}}(e^{j\hat{\omega}})$ in (66.39) on the same set of axes and then verify the result in (66.44b).

We can generalize the result of Example 66-6 in several interesting ways. First, we can see that when $\hat{\omega}_b > \hat{\omega}_{\text{CO}}$ the input (66.41) in a sense acts like an impulse to the ideal lowpass filter. That is, for ideal filters where a band of frequencies is zeroed out, many different inputs could produce the same output. Also, we can see that if the input to an ideal lowpass filter is any bandlimited signal such that $X(e^{j\hat{\omega}}) = 0$ for $\hat{\omega}_b < |\hat{\omega}| \leq \pi$ with $\hat{\omega}_b \leq \hat{\omega}_{\text{LP}}$, then the input signal will pass through the filter with no modification regardless of what $X(e^{j\hat{\omega}})$ is in the band $|\hat{\omega}| \leq \hat{\omega}_{\text{CO}}$. Finally, if the input consists of a desired signal plus some sort of competing signal such as noise whose spectrum extends over the entire range $|\hat{\omega}| \leq \pi$, then if the signal spectrum is concentrated in a band $|\hat{\omega}| \leq \hat{\omega}_b$, it follows by the principle of superposition that an ideal lowpass filter with cutoff frequency $\hat{\omega}_{\text{CO}} = \hat{\omega}_b$ will pass the signal without modification while removing all frequencies in the spectrum of the competing signal above the cutoff frequency. This is often the motivation for using a lowpass filter.

66-3.2 Ideal Highpass Filter

The ideal highpass filter has its stopband centered on low frequencies, and its passband extends from $|\omega| = \omega_{\text{CO}}$ out to $|\omega| = \pi$.

$$H_{\text{HP}}(e^{j\hat{\omega}}) = \begin{cases} 0 & |\hat{\omega}| \leq \hat{\omega}_{\text{CO}} \\ 1 & \hat{\omega}_{\text{CO}} < |\hat{\omega}| \leq \pi \end{cases} \tag{66.46}$$

Figure 66-4 shows an ideal HPF with its bandedge at ω_{CO} rad/s. In this case, the high frequency components of a signal will pass through the filter unchanged while the low frequencies will be completely eliminated. Like the ideal lowpass filter, we have defined the ideal highpass filter with conjugate symmetry so that $H_{\text{HP}}(e^{-j\hat{\omega}}) = H^*_{\text{HP}}(e^{j\hat{\omega}})$ so that the corresponding impulse response will be a real function of time.

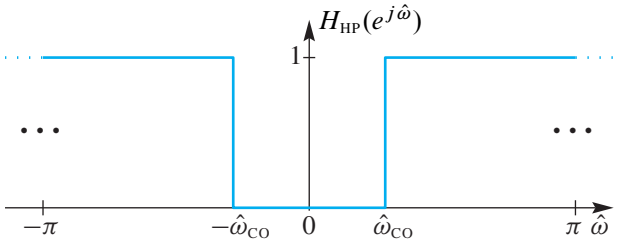

Figure 66-4: Frequency response of an ideal HPF with cutoff at ω_{CO} rad/s.

EXERCISE 66.8: If $H_{LP}(e^{j\hat{\omega}})$ is an ideal LPF with its bandedge at $\hat{\omega}_{CO}$ as plotted in Fig. 66-3, show that the frequency response of an ideal highpass filter with cutoff frequency $\hat{\omega}_{CO}$ can be represented by

$$H_{HP}(e^{j\hat{\omega}}) = 1 - H_{LP}(e^{j\hat{\omega}})$$

Hint: Try plotting the function $1 - H_{LP}(e^{j\hat{\omega}})$.

EXERCISE 66.9: Using the results of Exercise 66.8, show that the impulse response of the ideal highpass filter is

$$h_{CO}[n] = \delta[n] - \frac{\sin(\hat{\omega}_{CO}n)}{\pi n}$$

Highpass filters are often used to remove constant levels (DC) in sampled signals.

66-3.3 Ideal Bandpass Filter

The ideal bandpass filter has a passband centered away from the low frequency band, so it has two stopbands, one near DC and the other at high frequencies. Two bandedges must be given to specify the ideal BPF, ω_{CO_1} for the lower bandedge, and ω_{CO_2} for the upper bandedge.

$$H_{BP}(e^{j\hat{\omega}}) = \begin{cases} 0 & |\hat{\omega}| < \omega_{CO_1} \\ 1 & \hat{\omega}_{CO_1} \le |\hat{\omega}| \le \hat{\omega}_{CO_2} \\ 0 & \hat{\omega}_{CO_2} < |\hat{\omega}| \le \pi \end{cases} \tag{66.47}$$

Figure 66-5 shows an ideal BPF with its bandedges at $\hat{\omega}_{CO_1}$ and $\hat{\omega}_{CO_2}$. Once again we use a symmetrical definition of the passbands and stopbands which is required to make the corresponding impulse response real. In this case, all frequency components of a signal that lie in the band $\hat{\omega}_{CO_1} \le |\hat{\omega}| \le \hat{\omega}_{CO_2}$ are passed unchanged through the filter, while all other frequency components are completely removed.

EXERCISE 66.10: If $H_{BP}(e^{j\hat{\omega}})$ is an ideal BPF with its bandedges at $\hat{\omega}_{CO_1}$ and $\hat{\omega}_{CO_2}$, show by plotting that the filter defined by $H_{BR}(e^{j\hat{\omega}}) = 1 - H_{BP}(e^{j\hat{\omega}})$ could be called an ideal *band-reject* filter. Determine the edges of the stopband of the band-reject filter.

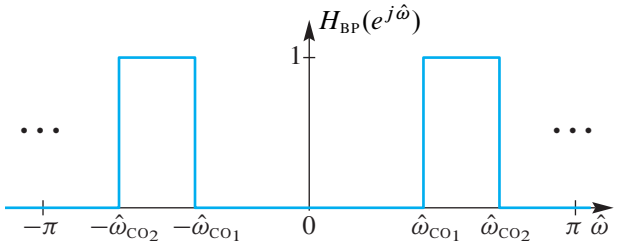

Figure 66-5: Frequency response of an ideal BPF with its passband from $\hat{\omega} = \hat{\omega}_{CO_1}$ to $\hat{\omega} = \hat{\omega}_{CO_2}$ rad/s.

66-4 Table of Fourier Transform Properties and Pairs

In this chapter, we have derived a number of useful transform pairs, and we have also derived several important properties of Fourier transforms. Table 66-1 on p. 20 includes the Fourier transform pairs that we have derived in this section as well as some transform pairs (such as for $u(t)$) that we did not derive.

Table 66-1: Basic discrete-time Fourier transform pairs.

Table of DTFT Pairs	
Time-Domain: $x[n]$	***Frequency-Domain:*** $X(e^{j\hat{\omega}})$
$\delta[n]$	1
$\delta[n-n_d]$	$e^{-j\hat{\omega}n_d}$
$u[n]-u[n-L]$	$\dfrac{\sin(\frac{1}{2}L\hat{\omega})}{\sin(\frac{1}{2}\hat{\omega})}\, e^{-j\hat{\omega}(L-1)/2}$
$\dfrac{\sin(\hat{\omega}_b n)}{\pi n}$	$u(\hat{\omega}+\hat{\omega}_b)-u(\hat{\omega}-\hat{\omega}_b) = \begin{cases} 1 & \lvert\hat{\omega}\rvert \le \hat{\omega}_b \\ 0 & \hat{\omega}_b < \lvert\hat{\omega}\rvert \le \pi \end{cases}$
$a^n u[n] \quad (\lvert a\rvert < 1)$	$\dfrac{1}{1-ae^{-j\hat{\omega}}}$
$b^n u[-n] \quad (\lvert b\rvert > 1)$	$\dfrac{1}{1-be^{-j\hat{\omega}}}$

The basic properties of the Fourier transform are what make it convenient to use in designing and analyzing systems, so they are given in Table 66-2 on p. 21 for easy reference.

Table 66-2: Basic discrete-time Fourier transform properties.

Table of DTFT Properties		
Property Name	***Time-Domain:*** $x[n]$	***Frequency-Domain:*** $X(e^{j\hat{\omega}})$
Periodic in $\hat{\omega}$		$X(e^{j(\hat{\omega}+2\pi)}) = X(e^{j\hat{\omega}})$
Linearity	$ax_1[n] + bx_2[n]$	$aX_1(e^{j\hat{\omega}}) + bX_2(e^{j\hat{\omega}})$
Conjugate Symmetry	$x[n]$ is real	$X(e^{-j\hat{\omega}}) = X^*(e^{j\hat{\omega}})$
Conjugation	$x^*[n]$	$X^*(e^{-j\hat{\omega}})$
Time-Reversal	$x[-n]$	$X(e^{-j\hat{\omega}})$
Delay	$x[n - n_d]$	$e^{-j\hat{\omega}n_d}X(e^{j\hat{\omega}})$
Frequency Shift	$x[n]e^{j\hat{\omega}_0 n}$	$X(e^{j(\hat{\omega}-\hat{\omega}_0)})$
Modulation	$x[n]\cos(\hat{\omega}_0 n)$	$\frac{1}{2}X(e^{j(\hat{\omega}-\hat{\omega}_0)}) + \frac{1}{2}X(e^{j(\hat{\omega}+\hat{\omega}_0)})$
Convolution	$x[n] * h[n]$	$X(e^{j\hat{\omega}})H(e^{j\hat{\omega}})$
Parseval's Theorem	$\sum_{n=-\infty}^{\infty} \lvert x[n]\rvert^2$	$\frac{1}{2\pi}\int_{-\pi}^{\pi} \lvert X(e^{j\hat{\omega}})\rvert^2 d\hat{\omega}$

66-5 Discrete Fourier Transform (DFT)

We have seen that the DTFT of a discrete-time signal $x[n]$ can be viewed as a generalization of the spectrum concept introduced in Chapters 3 and 4 which had discrete lines representing complex exponentials. The Fourier transform $X(e^{j\hat{\omega}})$ is a continuous spectrum for discrete-time signals $x[n]$. Because the spectrum is so useful, it is natural to want to be able to determine the spectrum of a signal even if it is not described by a simple mathematical formula. Indeed, it would be handy to have a computer program that could calculate the spectrum from samples of a signal.

Two steps are needed to change (66.4) into a computable form: the continuous frequency variable $\hat{\omega}$ must be sampled, and the limits on the sum must be finite. First, $\hat{\omega}$ is a continuous variable, but it does have a finite range $-\pi < \hat{\omega} \leq \pi$ so we can evaluate (66.4) at a finite set of frequencies, denoted by ω_k. Second, if the signal has infinite duration, we would have to take a finite section of the signal to make the sum have a finite number of terms in order to compute (66.4). For a finite-length signal the DTFT *sampled in frequency* becomes

$$X(e^{j\hat{\omega}_k}) = \sum_{n=0}^{L-1} x[n]e^{-j\omega_k n} \tag{66.48}$$

We must choose a finite set of frequencies $\{\omega_k\}$ for analysis, but which frequencies should be used to evaluate (66.48)? Although the usual domain for the spectrum is $-\pi < \hat{\omega} \leq \pi$, any interval of length 2π would suffice. For reasons that will become apparent, it is common to choose that interval to be

$$0 \leq \omega_k < 2\pi$$

and to evaluate (66.48) at the N equally spaced frequencies

$$\omega_k = \frac{2\pi k}{N} \qquad k = 0, 1, \ldots, N-1 \tag{66.49}$$

Substituting (66.49) into (66.48) leads to

$$X\left(e^{j\frac{2\pi k}{N}}\right) = \sum_{n=0}^{L-1} x[n]e^{-j(2\pi k/N)n} \tag{66.50}$$

for $k = 0, 1, \ldots, N-1$. Equation (66.50) is a finite "Fourier sum" which is computable. The sum in (66.50) must be computed for N different values of the discrete frequency index (k). Since the right-hand side of (66.50) depends only on k, we define $X[k] = X\left(e^{j\frac{2\pi k}{N}}\right)$.

When the number of frequency samples (N) is equal to the signal length (L), the summation in (66.50) with $N = L$ becomes:

The Discrete Fourier Transform

$$X[k] = \sum_{n=0}^{N-1} x[n]e^{-j(2\pi/N)kn} \qquad k = 0, 1, \ldots, N-1 \tag{66.51}$$

Equation (66.51) is called the ***discrete Fourier transform*** or ***DFT*** in recognition of the fact that it is a Fourier transformation, and it is discrete in both time and frequency. It takes N samples in the time-domain and *transforms* them into N values $X[k]$ in the frequency-domain. The values of both $x[n]$ and $X[k]$ can be complex. Since we have the same number of values in both domains, we expect the DFT to be invertible.

In addition, when we assume that $L = N$ in (66.51) very efficient algorithms exist for computing the N complex numbers specified by (66.51). These algorithms are collectively known as the ***fast Fourier transform*** or ***FFT***. In MATLAB, the computation of (66.51) is done by the function named `fft()`. We will have more to say about the FFT algorithm in Section 66-10.

A final comment is in order about the limits of summation in (66.51). We have chosen to sum over N samples of $x[n]$ and to evaluate the DFT at N frequencies. Often, the sequence $x[n]$ length is shorter than N, i.e., $L < N$, and $x[n]$ is nonzero only in the interval $0 \le n \le L-1$. In such cases, we can simply append $N-L$ zero samples to the nonzero samples of $x[n]$ and then carry out the N-point DFT computation.

Example 66-7: Short-Length DFT

In order to compute the 4-point DFT of the sequence $x[n] = \{1,\ 1,\ 0,\ 0\}$, we carry out the sum (66.51) for each value of $k = 0, 1, 2, 3$. When $N = 4$, all the exponents in (66.51) will be integer multiples of $\pi/2$ because $2\pi/N = \pi/2$.

$$\begin{aligned}
X[0] &= x[0]e^{-j0} + x[1]e^{-j0} + \cancelto{0}{x[2]}e^{-j0} + \cancelto{0}{x[3]}e^{-j0} \\
&= 1 + 1 + 0 + 0 = 2 \\
X[1] &= x[0]e^{-j0} + x[1]e^{-j\pi/2} + 0e^{-j\pi} + 0e^{-j3\pi/2} \\
&= 1 + (-j) + 0 + 0 = 1 - j = \sqrt{2}e^{-j\pi/4} \\
X[2] &= x[0]e^{-j0} + x[1]e^{-j\pi} + 0e^{-j2\pi} + 0e^{-j3\pi} \\
&= 1 + (-1) + 0 + 0 = 0 \\
X[3] &= x[0]e^{-j0} + x[1]e^{-j3\pi/2} + 0e^{-j3\pi} + 0e^{-j9\pi/2} \\
&= 1 + (j) + 0 + 0 = 1 + j = \sqrt{2}e^{j\pi/4}
\end{aligned}$$

Thus we obtain the four DFT coefficients[6] $X[k] = \{2,\ \sqrt{2}e^{-j\pi/4},\ 0,\ \sqrt{2}e^{j\pi/4}\}$. ■

66-5.1 The Inverse DFT

The DFT is a legitimate transform because it is possible to invert the transformation defined in (66.51). In other words, there exists an *inverse discrete Fourier transform* (or IDFT), which is a computation that converts $X[k]$ for $k = 0, 1, \ldots, N-1$ back into the sequence $x[n]$ for $n = 0, 1, \ldots, N-1$. The inverse DFT is

Inverse Discrete Fourier Transform

$$x[n] = \frac{1}{N}\sum_{k=0}^{N-1} X[k]e^{j(2\pi/N)kn} \qquad n = 0, 1, \ldots, N-1 \tag{66.52}$$

Equations (66.52) and (66.51) are the unique relationship between an N-point sequence $x[n]$ and its N-point DFT $X[k]$. Following our earlier terminology for Fourier representations, the DFT defined by (66.51) is the *analysis* equation and IDFT defined by (66.52) is the *synthesis* equation. To prove that these equations are a

[6] The term "coefficient" is commonly applied to DFT values. This is appropriate because $X[k]$ is the (complex amplitude) coefficient of $e^{j(2\pi/N)kn}$ in the IDFT (66.52).

consistent invertible Fourier representation, we note that (66.52), because it is a finite, well-defined computation, would surely produce *some* sequence when evaluated for $n = 0, 1, \ldots, N-1$. So let us call that sequence $v[n]$ until we prove otherwise. Part of the proof is given by the following steps:

$$\begin{aligned} v[n] &= \frac{1}{N}\sum_{k=0}^{N-1} X[k]e^{j(2\pi k/N)n} \\ &= \frac{1}{N}\sum_{k=0}^{N-1} \underbrace{\left(\sum_{m=0}^{N-1} x[m]e^{-j(2\pi k/N)m}\right)}_{\text{Forward DFT, } X[k]} e^{j(2\pi k/N)n} \\ &= \frac{1}{N}\sum_{m=0}^{N-1} x[m] \underbrace{\left(\sum_{k=0}^{N-1} e^{j(2\pi k/N)(n-m)}\right)}_{=0, \text{ except for } m=n} \\ &= x[n] \end{aligned} \tag{66.53}$$

Several things happened in the manipulations leading up to the equality assertion of (66.53). On the second line, we substituted the right-hand side of (66.51) for $X[k]$ after changing the index of summation from n to m. We are allowed to make this change because m is a "dummy index" that could be any symbol, and we need to reserve n for the index of the sequence $v[n]$ that is synthesized by the IDFT. On the third line, the summations on k and m were interchanged. This is permissible since these finite sums can be done in either order.

Now we need to consider the term in parenthesis in the third line of the proof. Exercise 66.11 states the required *orthogonality* result, which can be easily verified. If we substitute (66.55) into the third line of (66.53), we see that the only term in the sum on m that will be nonzero is the term corresponding to $m = n$. Thus $v[n] = x[n]$ for $0 \le n \le N-1$ as we wished to show.

EXERCISE 66.11: *Orthogonality Property of Periodic Discrete-Time Complex Exponentials*
Use the formula

$$\sum_{n=0}^{N-1} \alpha^n = \frac{1-\alpha^N}{1-\alpha} \tag{66.54}$$

to show that

$$\begin{aligned} d[m-k] &= \frac{1}{N}\sum_{n=0}^{N-1} e^{j(2\pi/N)mn} e^{j(2\pi/N)(-k)n} \quad \text{(definition)} \\ &= \frac{1}{N}\sum_{n=0}^{N-1} e^{j(2\pi/N)(m-k)n} \quad \text{(alternate form)} \\ &= \frac{1}{N}\left(\frac{1-e^{j(2\pi)(m-k)}}{1-e^{j(2\pi/N)(m-k)}}\right) \quad \text{(use (66.54))} \end{aligned}$$

$$d[m-k] = \begin{cases} 1 & m-k = rN \\ 0 & \text{otherwise} \end{cases} \tag{66.55}$$

where r is any positive or negative integer including $r = 0$.

Example 66-8: Short-Length IDFT

The 4-point DFT in Example 66-7 is $X[k] = \{2,\ \sqrt{2}e^{-j\pi/4},\ 0,\ \sqrt{2}e^{j\pi/4}\}$. If we compute the 4-point IDFT of the sequence $X[k]$, we should recover $x[n]$ when we apply the IDFT summation (66.52) for each value of $n = 0, 1, 2, 3$. As before, the exponents in (66.52) will all be integer multiples of $\pi/2$ when $N = 4$.

$$
\begin{aligned}
x[0] &= \tfrac{1}{4}\left(X[0]e^{j0} + X[1]e^{j0} + X[2]e^{j0} + X[3]e^{j0}\right) \\
&= \tfrac{1}{4}\left(2 + \sqrt{2}e^{-j\pi/4} + 0 + \sqrt{2}e^{j\pi/4}\right) = 1 \\
x[1] &= \tfrac{1}{4}\left(X[0]e^{j0} + X[1]e^{j\pi/2} + X[2]e^{j\pi} + X[3]e^{j3\pi/2}\right) \\
&= \tfrac{1}{4}\left(2 + \sqrt{2}e^{j(-\pi/4+\pi/2)} + 0 + \sqrt{2}e^{j(\pi/4+3\pi/2)}\right) = \tfrac{1}{4}(2 + (1+j) + (1-j)) = 1 \\
x[2] &= \tfrac{1}{4}\left(X[0]e^{j0} + X[1]e^{j\pi} + X[2]e^{j2\pi} + X[3]e^{j3\pi}\right) \\
&= \tfrac{1}{4}\left(2 + \sqrt{2}e^{j(-\pi/4+\pi)} + 0 + \sqrt{2}e^{j(\pi/4+3\pi)}\right) = \tfrac{1}{4}(2 + (-1+j) + (-1-j)) = 0 \\
x[3] &= \tfrac{1}{4}\left(X[0]e^{j0} + X[1]e^{j3\pi/2} + X[2]e^{j3\pi} + X[3]e^{j9\pi/2}\right) \\
&= \tfrac{1}{4}\left(2 + \sqrt{2}e^{j(-\pi/4+3\pi/2)} + 0 + \sqrt{2}e^{j(\pi/4+9\pi/2)}\right) = \tfrac{1}{4}(2 + (-1-j) + (-1+j)) = 0
\end{aligned}
$$

Thus we can recover the length-4 signal $x[n] = \{1,\ 1,\ 0,\ 0\}$ from its 4-point DFT coefficients, $X[k] = \{2,\ \sqrt{2}e^{-j\pi/4},\ 0,\ \sqrt{2}e^{j\pi/4}\}$. ■

66-5.2 Computing the DFT

The DFT representation in (66.51) and (66.52) is exceedingly important in digital signal processing for two reasons: the expressions have finite limits, making it possible to compute numeric values of $x[n]$ and $X[k]$, and they are Fourier representations that have special properties that are useful in the analysis and design of DSP systems. Both the DFT (66.51) and the IDFT summations (66.52) can be regarded simply as computational methods for taking N numbers in one domain and creating N numbers in the other domain. The values in both domains might be complex. Equation (66.51) is really N separate summations, one for each value of k. To evaluate one of the $X[k]$ terms, we need N complex multiplications and $N-1$ complex additions. If we count up all the arithmetic operations required to evaluate all of the $X[k]$ coefficients, the total is N^2 complex multiplications and $N^2 - N$ complex additions.

One of the most important discoveries[7] in the field of digital signal processing was the ***fast Fourier transform***, or ***FFT***, a set of algorithms that can evaluate (66.51) or (66.52) with a number of operations proportional to $N \log_2 N$ rather than N^2. When N is a power of two, the FFT algorithm computes the entire set of coefficients $X[k]$ with approximately $(N/2)\log_2 N$ complex operations. The $N \log_2 N$ behavior becomes increasingly significant for large N. For example, if $N = 1024$, the FFT will compute the DFT coefficients

[7] J. W. Cooley and J. W. Tukey, "An Algorithm for the Machine Computation of Complex Fourier Series," *Mathematics of Computation,* vol. 19, pp. 297–301, April 1965. The basic idea of the FFT has been traced back as far as Gauss at the end of the 18th Century.

$X[k]$ with $(N/2)\log_2 N = 5120$ complex multiplications, rather than $N^2 = 1{,}048{,}576$ as required by direct evaluation of (66.51). The algorithm is most often applied when the DFT length N is a power of two, but it also works efficiently if N has many small-integer factors. On the other hand, when N is a prime number, the standard FFT algorithm offers no savings over a direct evaluation of the DFT summation. FFT algorithms of many different variations are widely available in most computer languages, and for almost any computer hardware architecture. In MATLAB, the command is simply `fft`, and most other spectral analysis functions in MATLAB call `fft` to do the bulk of their work. More details on the FFT and its derivation can be found in Section 66-10 at the end of this chapter.

66-5.3 Matrix Form of the DFT and IDFT

Another easy way to gain insight into the computation is to write the DFT summation as a matrix multiplication:

$$\begin{bmatrix} X[0] \\ X[1] \\ X[2] \\ \vdots \\ X[N-1] \end{bmatrix} = \begin{bmatrix} 1 & 1 & 1 & \cdots & 1 \\ 1 & e^{-j2\pi/N} & e^{-j4\pi/N} & \cdots & e^{-j2(N-1)\pi/N} \\ 1 & e^{-j4\pi/N} & e^{-j8\pi/N} & \cdots & e^{-j4(N-1)\pi/N} \\ \vdots & \vdots & \vdots & \ddots & \vdots \\ 1 & e^{-j2(N-1)\pi/N} & e^{-j4(N-1)\pi/N} & \cdots & e^{-j2(N-1)(N-1)\pi/N} \end{bmatrix} \begin{bmatrix} x[0] \\ x[1] \\ x[2] \\ \vdots \\ x[N-1] \end{bmatrix} \tag{66.56}$$

In MATLAB, the DFT matrix can be obtained with the function `dftmtx(N)` for an $N \times N$ matrix. Then taking the DFT would be a matrix-vector product: `X = dftmtx(N)*x`. However, it is much more efficient to take the DFT of a vector using the statement `X = fft( x, N )`, where `x` is a vector of signal samples and `X` is the DFT of `x`. MATLAB uses a variety of FFT algorithms for this computation depending on the value of N with the best case being N equal to a power of 2.

EXERCISE 66.12: The IDFT can also be expressed as a matrix-vector product. Write out the typical entry of the $N \times N$ IDFT matrix, and then use MATLAB to create a 6×6 IDFT matrix. Check your work by multiplying the IDFT matrix by the DFT matrix (in MATLAB). The expected result should be an identity matrix.

66-6 Properties of the DFT

We will examine some special properties of the DFT that are tied to its origin as a frequency sampled version of the DTFT. Most DFT pairs and properties are inherited from the DTFT, but there are some exceptions such as the convolution property. One notable special property is the periodicity of $X[k]$ with respect to k which is inherited from the 2π-periodicity of the DTFT. This periodicity affects the placement of negative frequency components in $X[k]$, and also symmetries.

66-6.1 DFT Pairs and Properties from the DTFT

Since the DFT is a frequency sampled version of the DTFT for a finite-length signal, there is no need to have a special table containing DFT pairs. In Table 66-1, there are only three finite-length signals, so each of these has a DFT obtained by sampling $X(e^{j\hat{\omega}})$. The impulse signal is the easiest because

$$X[k] = \sum_{n=0}^{N-1} \delta[n] e^{-j(2\pi k/N)n} = \sum_{n=0}^{0} 1 e^{-j(2\pi k/N)n} = 1$$

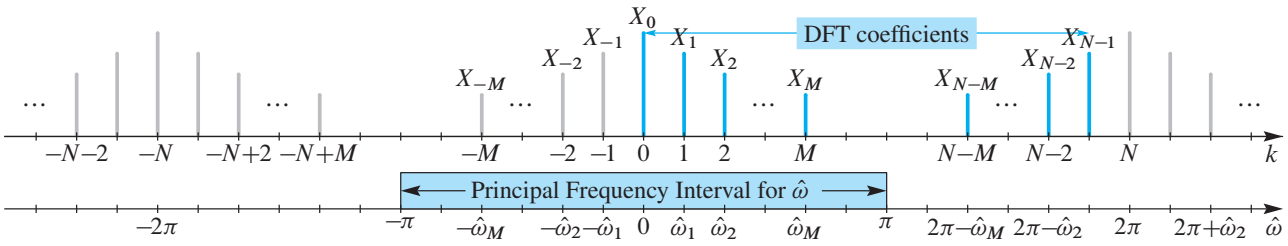

Figure 66-6: Periodicity of the DFT coefficients $X[k+N] = X[k]$, and the relationship of the frequency index k to samples of normalized frequency, $\hat{\omega}_k$. The DFT coefficients are denoted with subscripts, i.e., X_k instead of $X[k]$. The IDFT uses indexing that runs from $k = 0$ to $k = N-1$, which is one period. The DTFT, on the other hand, typically uses the principal frequency interval $-\pi \leq \hat{\omega} < \pi$.

This result is the same as the DTFT of $\delta[n]$. A more important case is the DFT of a finite-length (rectangular) pulse. If $p[n]$ is a length-L pulse

$$p[n] = \begin{cases} 1 & 0 \leq n \leq L-1 \\ 0 & L \leq n \leq N-1 \end{cases}$$

then

$$P[k] = P(e^{j\hat{\omega}})\Big|_{\hat{\omega}=(2\pi k/N)} = \frac{\sin(\frac{1}{2}L(2\pi k/N))}{\sin(\frac{1}{2}(2\pi k/N))}\, e^{-j(2\pi k/N)(L-1)/2}$$

66-6.2 DFT Periodicity for $X[k]$

Since the DTFT $X(e^{j\hat{\omega}})$ is always periodic with a period of 2π, the DFT $X[k]$ must also be periodic. The definition of the DFT implies that the index k always remains between 0 and $N-1$, but there is no reason that (66.51) cannot be evaluated for $k \geq N$, or $k < 0$. The frequency sampling relationship $\hat{\omega}_k = 2\pi k/N$ is still true for any integer k, so $\hat{\omega}_k + 2\pi = 2\pi k/N + 2\pi(N/N) = 2\pi(k+N)/N = \hat{\omega}_{k+N}$. In other words, the DFT coefficients $X[k]$ have a period equal to N, because

$$X[k] = X(e^{j2\pi(k)/N}) = X(e^{j(2\pi(k)/N+2\pi)}) = X(e^{j2\pi(k+N)/N}) = X[k+N]$$

When the DFT values $X[k]$ are used outside the interval $0 \leq k < N$, they must be extended with a period of N. Thus $X[N-1] = X[-1]$, $X[N-2] = X[-2]$, and so on. This periodicity is illustrated in Fig. 66-6.

66-6.3 Negative Frequencies and the DFT

The DFT and IDFT formulas use nonnegative indices, which is convenient for computation and mathematical expressions. As a result, the IDFT synthesis formula (66.52) appears to have positive frequencies only. However, when we make the spectrum plot of a discrete-time signal (as in Chapter 4, Figs. 4-8 through 4-11) we expect to see both positive and negative frequency lines, along with conjugate symmetry when the signal is real. Thus we must study how to use the DFT to produce a conjugate-symmetric spectrum plot.

The signal defined by the IDFT in (66.52) has N equally spaced normalized frequencies $\hat{\omega}_k = (2\pi/N)k$ over the positive frequency range $[0, 2\pi)$. These frequencies can be separated into two subsets

$$0 \leq (2\pi/N)k < \pi \quad \text{for} \quad 0 \leq k < N/2 \tag{66.57a}$$

$$\pi \leq (2\pi/N)k < 2\pi \quad \text{for} \quad N/2 \leq k \leq N-1 \tag{66.57b}$$

Since the DTFT is periodic in $\hat{\omega}$ with a period of 2π, the sample of the DTFT at $\hat{\omega}_k = (2\pi/N)(-k)$ has the same value as the sample at frequency $\hat{\omega}_{N-k} = (2\pi/N)(-k+N)$. This is aliasing. In other words, the index $k = N-1$ corresponding to the positive frequency $\hat{\omega}_{N-1} = 2\pi(N-1)/N$ aliases to the index $k = -1$ which corresponds to $\hat{\omega}_{-1} = -2\pi/N = \hat{\omega}_{N-1} - 2\pi$. In fact, all the frequencies in the second subset above (66.57b) actually alias to the negative frequencies in the spectrum.[8] This is important when we want to plot the spectrum for $-\pi \leq \hat{\omega} < \pi$. When N is even, the indices in the second subset $\{\frac{N}{2}, \frac{N}{2}+1, \frac{N}{2}+2, \ldots, N-2, N-1\}$ would be aliased to $\{-\frac{N}{2}, -\frac{N}{2}+1, -\frac{N}{2}+2, \ldots, -2, -1\}$.

EXERCISE 66.13: Prove that the IDFT can be rewritten as a sum where half the indices are negative. Assume that the DFT length N is even.

$$x[n] = \frac{1}{N} \sum_{k=-N/2}^{N/2-1} X[k] e^{j(2\pi/N)kn}$$

66-6.3.1 Conjugate Symmetry of the DFT

When we have a real signal $x[n]$, there is conjugate symmetry in the DTFT, so the DFT coefficients also satisfy the following property: $X[-1] = X^*[1]$, $X[-2] = X^*[2]$. If we put the periodicity of $X[k]$ together with conjugate symmetry, we can make the general statement that the DFT of a real signal satisfies

$$X[N-k] = X^*[k] = X[-k] \quad \text{for } k = 0, 1, \ldots, N-1$$

Figure 66-7 shows a DFT coefficient $X[k_0]$ at the normalized frequency $\hat{\omega}_{k_0} = 2\pi k_0/N$. The corresponding negative-frequency component is shown in gray at $k = -k_0$. The spectrum component at $k = N - k_0$ is an alias of the negative-frequency component.

Example 66-9: DFT Symmetry

In Example 66-7, the frequency indices of the 4-pt. DFT correspond to the four frequencies $\hat{\omega}_k = \{0, \pi/2, \pi, 3\pi/2\}$. The frequency $\hat{\omega}_3 = 3\pi/2$ is an alias of $\hat{\omega} = -\pi/2$. We can check that the DFT coefficients in Example 66-7 satisfy the conjugate-symmetric property, e.g., $X[1] = X^*[4-1] = X^*[3] = \sqrt{2}e^{-j\pi/4}$. ■

EXERCISE 66.14: It is easy to create a MATLAB example that demonstrates the conjugate-symmetry property by executing `Xk=fft(1:8)`, which computes the 8-pt. DFT of a real signal. List the values of the signal $x[n]$ for $n = 0, 1, 2, \ldots, 7$. Then tabulate the values of the MATLAB vector `Xk` in polar form from which you can verify that $X[N-k] = X^*[k]$ for $k = 0, 1, \ldots, 7$. Finally, list the value of $\hat{\omega}$ corresponding to each index k.

[8] The case where $k = N/2$ and N is even will be discussed further in Sect. 66-6.3.2. We follow the MATLAB convention (when using `fftshift`) that puts this index in the second set.

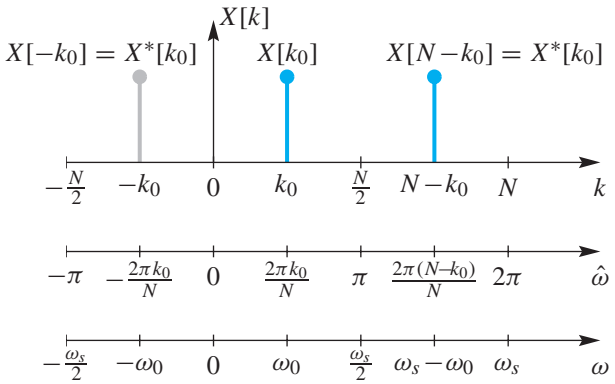

Figure 66-7: Illustration of the conjugate-symmetry of the DFT coefficients showing that $X[N-k_0] = X^*[k_0]$. There are three "frequency scales." The top scale shows the DFT index k. The middle scale shows normalized frequency $\hat{\omega}$ for the discrete-time signal. The bottom scale shows the continuous-time frequency scale ($\omega = \hat{\omega}/T_s$) that would be appropriate if the sequence $x[n]$ had been obtained by sampling with a sampling frequency, $\omega_s = 2\pi/T_s$. Thus the DFT index k_0 corresponds to the analog frequency $\omega_0 = 2\pi k_0/(NT_s)$ rad/s.

66-6.3.2 Ambiguity at $X[N/2]$

When the DFT length N is even, the transform $X[k]$ has a value at $k = N/2$; when N is odd, $k = N/2$ is not an integer so the following comments do not apply. The index $k = N/2$ corresponds to a normalized frequency of $\hat{\omega} = 2\pi(N/2)/N = \pi$. However, the spectrum is periodic in $\hat{\omega}$ with a period of 2π, so the spectrum value is the same at $\hat{\omega} = \pm\pi$. In other words, the frequency $\hat{\omega} = -\pi$ is an alias of $\hat{\omega} = \pi$.

When we plot a spectrum as in Chapter 3, the zero frequency line is placed in the middle, and the frequency axis runs from $-\pi$ to $+\pi$. Strictly speaking we need not include both end points because the values have to be equal, $X[N/2] = X[-N/2]$. Thus, we have to make a choice, either placing $X[N/2]$ on the positive frequency side, or $X[-N/2]$ on the negative frequency side of the spectrum. The following example for $N = 6$ shows the two re-orderings that are possible:

$$\{\underbrace{X[0]}_{\hat{\omega}=0}, X[1], X[2], \underbrace{X[3]}_{\hat{\omega}=\pi}, X[4], X[5]\} \longrightarrow \{\underbrace{X[-3]}_{\hat{\omega}=-\pi}, X[-2], X[-1], \underbrace{X[0]}_{\hat{\omega}=0}, X[1], X[2]\}$$

$$\longrightarrow \{X[-2], X[-1], \underbrace{X[0]}_{\hat{\omega}=0}, X[1], X[2], \underbrace{X[3]}_{\hat{\omega}=\pi}\}$$

In this example, the periodicity of the DFT coefficients enabled the following replacements $X[5] = X[-1]$, $X[4] = X[-2]$, and $X[3] = X[-3]$. The DFT component $X[3]$ at $k = 3$ corresponding to the frequency $\hat{\omega} = 2\pi(3)/6 = \pi$ is the same as $X[-3]$ at $k = -3$ corresponding to $\hat{\omega} = 2\pi(-3)/6 = -\pi$. The choice of which reordering to use is arbitrary, but the MATLAB function `fftshift` does the first, putting $X[N/2]$ at the beginning so that it becomes $X[-N/2]$ and corresponds to $\hat{\omega} = -\pi$. Therefore, we adopt this convention in this chapter.

EXERCISE 66.15: Prove that the DFT coefficient $X[N/2]$ must be real-valued when the vector $x[n]$ is real and the DFT length N is even.

66-6.4 Frequency Domain Sampling and Interpolation

When we want to make a smooth plot of a DTFT such as the frequency response, we need frequency samples at a very fine spacing. Implicitly, the DFT assumes that the transform length is the same as the signal length L. Thus the L-point DFT *computes samples of the* DTFT for $\hat{\omega} = (2\pi/L)k$, with $k = 0, 1, \ldots, L-1$; i.e., for L equally spaced samples of $\hat{\omega}$ in $[0, 2\pi)$.

$$H[k] = H(e^{j(2\pi/L)k}) = H(e^{j\hat{\omega}})\Big|_{\hat{\omega}=(2\pi/L)k} \qquad k = 0, 1, \ldots, L-1 \tag{66.58}$$

If we want to have frequency samples at a finer spacing $(2\pi/N)$ where $N > L$, then a simple trick can be used to make an N-point DFT: ***zero-padding***, i.e, append zeros to the signal to make it longer prior to taking the N-point DFT. In other words, define a length-N signal $h_{\text{zp}}[n]$ as

$$h_{\text{zp}}[n] = \begin{cases} h[n] & n = 0, 1, \ldots, L-1 \\ 0 & n = L, L+1, \ldots, N-1 \end{cases} \tag{66.59}$$

Now take the N-point DFT of $h_{\text{zp}}[n]$ and then split the sum into two smaller summations:

$$H_{\text{zp}}[k] = \sum_{n=0}^{N-1} h_{\text{zp}}[n] e^{-j(2\pi/N)kn} \tag{66.60}$$

$$= \sum_{n=0}^{L-1} h_{\text{zp}}[n] e^{-j(2\pi/N)kn} + \sum_{n=L}^{N-1} \cancelto{0}{h_{\text{zp}}[n]} e^{-j(2\pi/N)kn} \tag{66.61}$$

$$= \sum_{n=0}^{L-1} h[n] e^{-j(2\pi/N)kn} \tag{66.62}$$

$$H_{\text{zp}}[k] = H(e^{j(2\pi/N)k}) \qquad \text{for } k = 0, 1, 2, \ldots, N-1 \tag{66.63}$$

Thus (66.63) says the N-point DFT of an L-point (impulse response) signal with zero padding will give frequency response samples at $\hat{\omega}_k = 2\pi k/N$.

In the special case where $N = 2L$, we get twice as many frequency samples as with $N = L$, but the even-indexed samples are identical to values that we had before, i.e.,

$$H_{\text{zp}}[2\ell] = H[\ell] \qquad \text{for } \ell = 0, 1, \ldots, L-1 \tag{66.64}$$

Consider an even-indexed frequency such as $(2\pi/N)10$ when $N = 2L$. The frequency $(2\pi/2L)10 = (2\pi/L)5$, i.e., the tenth value of $H_{\text{zp}}[k]$, is the same as the fifth value of $H[k]$ because these values come from evaluating $H(e^{j\hat{\omega}})$ at exactly the same frequency. On the other hand, consider an odd-indexed frequency such as $(2\pi/N)7$ when $N = 2L$. Then the frequency $(2\pi/2L)7 = (2\pi/L)(3.5)$ lies between $(2\pi/L)3$ and $(2\pi/L)4$, so the odd-indexed frequencies correspond to evaluating the frequency response "in between." In other words, the $2L$-point DFT is *interpolating* $H[k]$ which has L sample values of the frequency response. Once we recognize this interpolation behavior of the DFT, we can use even more zero-padding to produce very dense frequency grids for evaluating the frequency response prior to plotting. In fact, in the limit as $N \to \infty$, the DFT will converge to the true frequency response function which is a continuous function of $\hat{\omega}$.

Example 66-10: Frequency Response Plotting with DFT

Suppose that we want to plot the frequency response of an 11-point averager, which is an FIR filter. Although MATLAB can do the job with its frequency response function called `freqz`, we can also do the evaluation directly with the DFT by calling `fft` in MATLAB. This will provide insight into the internal structure of `freqz` which calls the FFT to do the actual work. To evaluate the frequency response at many closely spaced frequencies we need to use zero padding, so we pick $N = 200$ and do the following in MATLAB.

```
N = 200;
xpadded = [ (1/11)*ones(1,11), zeros(1,N-11) ];
Xk = fft(xpadded);
plot( 0:N-1, abs(Xk))
```

Zero-padding is a very common operation, so the `fft` function has a second argument that sets the FFT length. Thus, `fft(xx,N)` takes an N-point DFT of `xx`, with zero-padding if necessary.

If we compare the plot from this code to the magnitude plot in Fig. 6-9, we see that the result is very close, but there is a big issue: the frequency axis needs to have $\hat{\omega}$ running from $-\pi$ to π. The negative frequency components must be moved as explained in Sect. 66-6.3 and the axis labels must be converted from "frequency index" to $\hat{\omega}$. This is accomplished by treating the second half of the `Xk` vector different from the first half as in the following code (which assumes `N` is even).

```
XkCentered = [ Xk(N/2+1:N), Xk(1:N/2) ]; %- fftshift.m will do this
kCentered =  [-N+(N/2+1:N),   (1:N/2) ] - 1;  %- make negative frequency indices
                    % kCentered will be [-N/2,-N/2+1,...,-2,-1,0,1,2,3,...,N/2-1]
plot( (2*pi/N)*kCentered, abs(XkCentered))
```

The flipping operation above occurs so often when using the FFT in MATLAB that a special function called `fftshift` has been created to perform the reordering. The frequencies have to be done separately. When the frequency response has conjugate symmetry, it is customary to plot only the first half of `Xk` which corresponds to the positive frequency region. ■

66-6.5 DFT of a Complex Exponential

The DFT transforms a time-domain signal into its frequency-domain representation, but the transform is usually a *numerical operation* that takes a vector of time samples and produces a vector of DFT coefficient values. However, in some important special cases, the finite sum can be "summed analytically" to obtain a simple formula for the DFT coefficients. One such example is the DFT of a finite-length complex exponential which is an important case for spectrum analysis where signals are represented as sums of complex exponentials.

Consider a finite section of a general complex exponential

$$x_1[n] = Ae^{j(\hat{\omega}_0 n+\varphi)} \qquad \text{for } n = 0, 1, 2, \ldots, L-1$$

whose length is L. An alternative representation for $x_1[n]$ is the product of a length-L rectangular pulse times, the complex exponential.

$$x_1[n] = Ae^{j(\hat{\omega}_0 n+\varphi)}\, r_L[n]$$

where the rectangular pulse $r_L[n] = u[n]-u[n-L]$ is equal to one for $n = 0, 1, 2, \ldots, L$–1, and zero elsewhere.

To determine an expression for the DFT, we first find the DTFT of $x_1[n]$ and then frequency sample $X_1(e^{j\hat{\omega}})$. The DTFT of $r_L[n]$ is known from Table 66-1; it consists of a Dirichlet form times a complex

exponential. Thus the DTFT of $x_1[n]$ will be obtained with the frequency shifting property:

$$X_1(e^{j\hat{\omega}}) = = Ae^{j\varphi}\ R_L(e^{-j(\hat{\omega}-\hat{\omega}_0)}) \tag{66.65}$$

$$= Ae^{j\varphi}\, D_L(\hat{\omega}-\hat{\omega}_0)\, e^{-j(\hat{\omega}-\hat{\omega}_0)(L-1)/2} \tag{66.66}$$

where $D_L(\hat{\omega}-\hat{\omega}_0)$ is a shifted version of the Dirichlet function[9]

$$D_L(\hat{\omega}) = \frac{\sin(\hat{\omega}L/2)}{\sin(\hat{\omega}/2)} \tag{66.67}$$

Notice that, in deriving this result, we have not yet exploited any special information about the frequency $\hat{\omega}_0$, such as $\hat{\omega}_0$ being equal to an integer multiple of $2\pi/N$ which will lead to a very simple result when $L = N$. Now we perform frequency sampling to get the DFT from the DTFT, and the final result is

$$X_1[k] = Ae^{j\varphi}\ D_L((2\pi k/N)-\hat{\omega}_0)\, e^{-j((2\pi k/N)-\hat{\omega}_0)(L-1)/2} \tag{66.68}$$

Since the exponential terms in (66.68) only contribute to the phase, this result says that the magnitude $|X_1[k]| = A|D_L((2\pi k/N)-\hat{\omega}_0)|$ is a scaled, and sampled, and shifted Dirichlet function. A typical magnitude plot of $|X[k]|$ is shown in Fig. 66-8 for the case when $N = L = 20$, $\hat{\omega}_0 = 5\pi/20 = 2\pi(2.5)/N$, and $A = 1$. The continuous magnitude of the Dirichlet function (for the DTFT) has been plotted in gray so that it is obvious where the frequency samples are being taken. Notice that the peak of the Dirichlet envelope lies along the horizontal axis at the non-integer value of 2.5, which is also $\hat{\omega} = (2\pi/N)(2.5)$ for the DTFT.

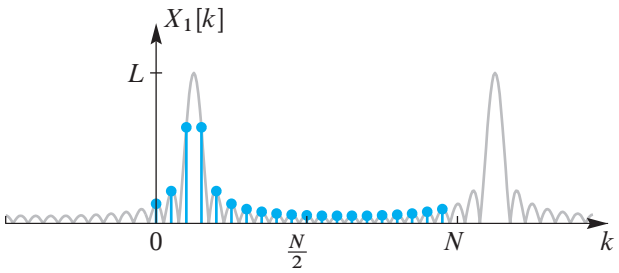

Figure 66-8: DFT of a complex exponential whose frequency is *not an integer multiple of* $2\pi/N$ with $N = L = 20$.

When the frequency of the signal $x_1[n]$ is an exact integer multiple of $2\pi/N$ and there is no zero-padding (i.e., $L = N$), the resulting DFT becomes very simple. For this special case, we define $x_2[n] = e^{j(2\pi k_0/N)n}$ with $k_0 < N$, and then use $\hat{\omega}_0 = 2\pi k_0/N$ and $Ae^{j\varphi} = 1$ in (66.68) to obtain

$$X_2[k] = D_N(2\pi(k-k_0)/N)\ e^{-j(2\pi(k-k_0)/N))(N-1)/2}$$

The big simplification comes from the fact that the Dirichlet $D_N(\hat{\omega})$ evaluated at integer multiples of $2\pi/N$ is zero, except for $D_N(0)$, so we get

$$X_2[k] = N\delta[k-k_0] \tag{66.69}$$

The scaled discrete impulse at $k = k_0$ means that $X_2[k_0] = N$ and all other DFT coefficients are zero. This result is confirmed in Fig. 66-9, where we can see that the DFT $X_2[k]$ is obtained by sampling the Dirichlet

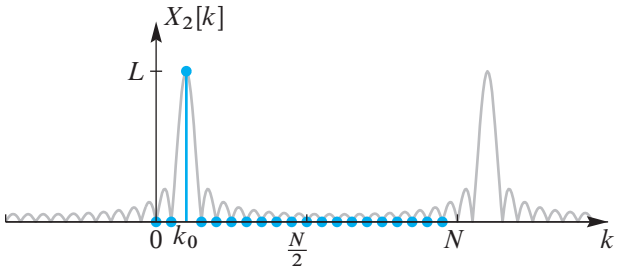

Figure 66-9: DFT of a complex exponential whose frequency *is an integer multiple* of $2\pi/N$; i.e., $N = L = 20$ and $k_0 = 2$.

function envelope exactly at its peak and at its zero crossings. The peak value is N, and it is the only nonzero value in the DFT.

EXERCISE 66.16: Substitute (66.69) into the inverse N-point DFT relation (66.52) to show that the corresponding time-domain sequence is

$$x_2[n] = e^{j(2\pi/N)k_0 n} \qquad n = 0, 1, \ldots, N-1$$

EXERCISE 66.17: Use Euler's relation to represent the signal $x_3[n] = A\cos(2\pi k_0 n/N)$ as a sum of two complex exponentials. Assume k_0 is an integer. Use the fact that the DFT is a linear operation to show that

$$X_3[k] = \frac{AN}{2}\delta[k - k_0] + \frac{AN}{2}\delta[k + k_0]$$

or, equivalently,

$$X_3[k] = \frac{AN}{2}\delta[k - k_0] + \frac{AN}{2}\delta[k - (N - k_0)]$$

66-6.6 DFT of a Real Cosine Signal

The examples shown in Figs. 66-8 and 66-9 assume that $N = L$; i.e., the DFT length N is equal to the length of the complex exponential sequence. However, the general result in (66.68) holds for $L \leq N$, and it is useful to examine the case where $L < N$. Consider a length-L cosine signal

$$x_4[n] = A\cos(\hat{\omega}_0 n) \qquad \text{for } n = 0, 1, \ldots, L-1 \tag{66.70a}$$

which we can write as the sum of complex exponentials at frequencies $+\hat{\omega}_0$ and $-\hat{\omega}_0$ as follows:

$$x_4[n] = \frac{A}{2}e^{j\hat{\omega}_0 n} + \frac{A}{2}e^{-j\hat{\omega}_0 n} \qquad \text{for } n = 0, 1, \ldots, L-1 \tag{66.70b}$$

[9] The Dirichlet function was first defined in Section 6-7 on p. 142.

Using the linearity of the DFT and (66.68) with $\varphi = 0$ for these two frequencies leads to the expression

$$\begin{aligned} X_4[k] &= \frac{A}{2} D_L((2\pi k/N) - \hat{\omega}_0)\, e^{-j((2\pi k/N)-\hat{\omega}_0)(L-1)/2} \\ &\quad + \frac{A}{2} D_L((2\pi k/N) + \hat{\omega}_0)\, e^{-j((2\pi k/N)+\hat{\omega}_0)(L-1)/2} \end{aligned} \tag{66.71}$$

where the function $D_L(\hat{\omega})$ is given by (66.67).

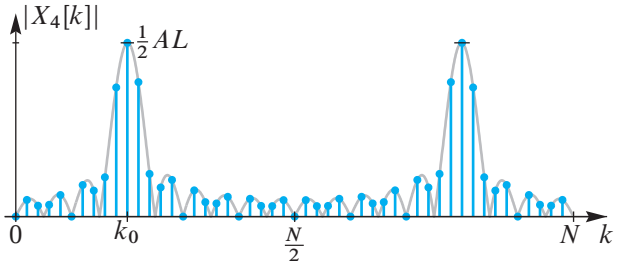

Figure 66-10: N-point DFT of a length-L real cosine signal whose frequency is an integer multiple of $2\pi/N$, where $N = 50$ and $L = 20$. The integer multiple is $k_0 = 10$, so $\hat{\omega}_0 = (2\pi/50)10 = 0.2\pi$.

Figure 66-10 shows $|X_4[k]|$ as a function of k for the case $\hat{\omega}_0 = 0.2\pi$ with $N = 50$ and $L = 20$. An equivalent horizontal axis would be the normalized frequency axis ($\hat{\omega}$) where $\hat{\omega}_k = 2\pi k/N$. Note the DFT magnitude exhibits its characteristic symmetry where the maxima (peaks) of the DFT occur for values of k and $N - k$, i.e., at frequencies $(2\pi k_0/N) = \hat{\omega}_0$ and $(2\pi(N - k_0)/N) = 2\pi - \hat{\omega}_0$. Furthermore, the heights of the peaks are approximately $AL/2$. The latter can be shown by evaluating (66.71) under the assumption that $(2\pi k_0/N) = \hat{\omega}_0$ and that the value of $|X_4[k_0]|$ is determined mainly by the first term in (66.71).

In Section 66-9, we will revisit the fact that isolated spectral peaks are often indicative of sinusoidal signal components. Knowledge of the fact that the peak height depends on both the amplitude A and the duration L will be useful in interpreting spectrum analysis results for signals involving multiple frequencies.

EXERCISE 66.18: Use MATLAB to compute samples of the signal $x_0[n] = 5\cos(0.211\pi n)$ for $n = 0, 1, \ldots, 499$. Compute and plot the magnitude of the $(N = 16384)$-point DFT of the length-500 sequence $x_0[n]$ using the MATLAB statements

```
x0=5*cos( 0.211*pi*(0:499) );
N=16384;
X0 = fft(x0,N);   %- fft will take care of zero padding
plot( (0:N/2)*2*pi/N , abs(X0(1:N/2+1) );
```

Check to see if the peak height satisfies the relation $AL/2$ mentioned above.
Repeat the above steps for the following length-5000 input signal

$$x_3[n] = \begin{cases} 0.5\cos(0.4\pi n) & \text{for } n = 5000, 5001, \ldots, 9999 \\ 0 & \text{otherwise} \end{cases}$$

Overlay the two plots by musing MATLAB's `hold on` command before plotting the second DFT. Explain why the spectral peak height is the same for both signals even though their amplitudes differ by a factor of ten.

66-7 Discrete-Time Spectrum Analysis

In Chapter 3, Section 3-6, the Fourier Series integral was presented as the operator that "Fourier analyzes" a continuous-time *periodic signal* to extract its spectrum. In this section, we will consider the Discrete Fourier Series (DFS) representation of a discrete-time signal that is periodic. The key to this is the IDFT sum which will synthesize a periodic signal when evaluated outside of the $0 \le n \le N-1$ interval. As a result, we will develop a method of Fourier analysis that uses the DFT to extract the spectrum of a discrete-time (sampled) periodic signal $\tilde{x}[n]$ by taking the DFT of one period of its samples. Then we will be able to connect the spectrum analysis of a periodic discrete-time signal to the spectrum of a periodic continuous-time signal.[10]

66-7.1 Periodic Discrete-time Signal: Fourier Series

The signal $\tilde{x}[n]$ is periodic if it repeats with an *integer* period of N samples, i.e., $\tilde{x}[n+N] = \tilde{x}[n]$. We use the tilde $\tilde{x}$ to emphasize that the signal is periodic. In this case, we can take the DFT of N values taken from one period of the signal $\{\tilde{x}[0],\ \tilde{x}[1],\ \ldots \tilde{x}[N-1]\}$

$$\tilde{X}[k] = \sum_{n=0}^{N-1} \tilde{x}[n] e^{-j(2\pi k/N)n} \tag{66.72}$$

The IDFT of $\tilde{X}[k]$ gives a representation for $\tilde{x}[n]$ which seems to be valid only for $0 \le n \le N-1$.

$$\tilde{x}[n] = \frac{1}{N} \sum_{k=0}^{N-1} \tilde{X}[k] e^{j(2\pi k/N)n} \qquad \text{for } n = 0, 1, 2, \ldots, N-1. \tag{66.73}$$

However, it turns out that this summation is also a valid representation for $\tilde{x}[n]$ for all time indices, $-\infty < n < \infty$, because we can show that $\tilde{x}[n]$ defined by (66.73), when evaluated outside the interval $0 \le n \le N-1$, must be periodic, satisfying $\tilde{x}[n+N] = \tilde{x}[n]$. The justification is as follows:

$$\tilde{x}[n+N] = \frac{1}{N} \sum_{k=0}^{N-1} \tilde{X}[k] e^{j(2\pi k/N)(n+N)} = \overbrace{\frac{1}{N} \sum_{k=0}^{N-1} \tilde{X}[k] e^{j(2\pi k/N)n}}^{\tilde{x}[n]} \underbrace{e^{j(2\pi k/N)(N)}}_{\to 1} \tag{66.74}$$

Another notable fact about the IDFT summation (66.73) is that it is the sum of N complex exponentials with uniformly spaced frequencies, $\hat{\omega}_k = (2\pi/N)k$. Thus, we can call this representation (66.73) the *Discrete Fourier Series* because we have a representation of a discrete-time periodic signal as a sum of harmonic complex exponentials. Recall that the Fourier Series synthesis formula for continuous-time signals (given in Ch. 3) represents a periodic signal as a (possibly infinite) sum of harmonic complex exponentials.

When the signal is real-valued, e.g., a sinusoid, then we would expect a synthesis formula with negative frequencies, as well as positive frequencies, e.g.,

$$\tilde{x}[n] = \sum_{m=-M}^{M} a_m e^{j(2\pi m/N)n} \qquad \text{for } -\infty < n < \infty. \tag{66.75}$$

[10] Later we will develop the continuous-time Fourier transform (CTFT) and show that the same relationship holds between the DTFT and CTFT.

where the coefficients $\{a_m\}$ have complex conjugate symmetry, $a_{-m} = a_m^*$. In the discrete-time case, the summation limit (M) must be finite because (66.73) is a general representation for any periodic discrete-time signal whose period is N, and the sum in (66.73) has only N terms. The number of terms in (66.75) is $2M+1$, so we must have $2M \leq N-1$.

Example 66-11: Synthesize a Periodic Signal

Suppose that a signal $\tilde{x}[n]$ is defined with a DFS summation like (66.75) with specific values for the coefficients $a_m = (m^2 - 1)$, i.e.,

$$\tilde{x}[n] = \sum_{m=-2}^{2} (m^2 - 1) e^{j(2\pi/N)mn} \qquad \text{for } -\infty < n < \infty.$$

If $N = 5$, make a list of the values of $\tilde{x}[n]$ for $m = 0, 1, 2, \ldots, 10$ to show that $\tilde{x}[n]$ has a period equal to 5. ■

The coefficients of the complex exponential terms $(1/N)\tilde{X}[k]$ in (66.73) will become the Fourier Series coefficients. We already know that the DFT coefficients are periodic, i.e., $\tilde{X}[k \pm N] = \tilde{X}[k]$ as shown in Fig. 66-6. Thus we can identify the coefficients in (66.75) with respect to those in (66.73) to obtain

$$a_m = \begin{cases} \frac{1}{N}\tilde{X}[m] & m = 0, 1, 2, \ldots, M \\ \frac{1}{N}\tilde{X}[m+N] & m = -1, -2, \ldots, -M \end{cases} \tag{66.76}$$

The end result is that we can write a Discrete Fourier Series (DFS) for a periodic discrete-time signal by using the (scaled) DFT as an analysis summation to obtain the $\{a_m\}$ coefficients from one period of the signal.

$$a_k = \frac{1}{N} \sum_{n=0}^{N-1} \tilde{x}[n] e^{-j(2\pi k/N)n} \tag{66.77a}$$

$$\tilde{x}[n] = \sum_{k=0}^{N-1} a_k e^{j(2\pi k/N)n} = \sum_{k=-M}^{M} a_k e^{j(2\pi k/N)n} \qquad (\text{for } 2M+1 \leq N) \tag{66.77b}$$

In this case, the factor of $(1/N)$ is associated with the analysis summation (66.77a).

Example 66-12: DFS Coefficients

There are two cases to consider: N even and N odd. The notation is much easier when N is odd because we can write $N = 2M+1$ where M is an integer. For example, when $N = 5$ we have $M = 2$, so the Fourier Series would be

$$\tilde{x}[n] = a_0 + a_1 e^{j0.4\pi n} + a_2 e^{j0.8\pi n} + a_{-1} e^{-j0.4\pi n} + a_{-2} e^{-j0.8\pi n}$$

On the other hand, when N is even there is a complication. When $N = 4$ the summation in (66.75) implies that $2M \leq 3$, or $M = 1$, but using the 4-pt DFT we can write

$$\tilde{x}[n] = a_0 + a_1 e^{j0.5\pi n} + a_2 e^{j\pi n} + a_{-1} e^{-j0.5\pi n}$$

The case where $a_2 \neq 0$ is a special case that is similar to the ambiguity with $X[N/2]$ treated in Sect. 66-6.3.2. The value of a_2 (or $X[N/2]$) will be real when the signal is real, so it does not require a complex conjugate term in negative frequency.

■

Example 66-13: Period of a discrete-time sinusoid

We might expect the fundamental period of a periodic signal to be the inverse of its fundamental frequency because this is true for continuous-time signals. However, for discrete-time signals this fact is often not true. The reason for this uncertainty is the requirement that *the period of the discrete-time signal be an integer.*

Consider the signal $\tilde{x}_1[n] = \cos(0.125\pi n)$, whose frequency is $\pi/8$ rads. The period of this signal is $N = 16$; it is also the shortest period so maybe we want to call it the fundamental period. If we take the 16-pt. DFT of one period of $\tilde{x}_1[n]$ we get $\tilde{X}_1[k] = 8\delta[k-1] + 8\delta[k-15]$. Then we can convert these DFT coefficients into a DFS representation with $a_1 = 8/16 = \frac{1}{2}$ and $a_{-1} = 8/16 = \frac{1}{2}$

$$\tilde{x}_1[n] = \tfrac{1}{2}e^{j(2\pi/16)n} + \tfrac{1}{2}e^{j(2\pi(-1)/16)n}$$

Now, consider the signal $\tilde{x}_2[n] = \cos(0.625\pi n)$, whose frequency is $5\pi/8$ rads. Its period is also $N = 16$, and this is the shortest period. If we take the 16-pt. DFT of one period of $\tilde{x}_2[n]$ we get $\tilde{X}_2[k] = 8\delta[k-5] + 8\delta[k-11]$. Then we can convert these DFT coefficients into a DFS representation with $a_5 = 8/16 = \frac{1}{2}$ and $a_{-5} = 8/16 = \frac{1}{2}$

$$\tilde{x}_2[n] = \tfrac{1}{2}e^{j(2\pi(5)/16)n} + \tfrac{1}{2}e^{j(2\pi(-5)/16)n}$$

The problem facing us is that a_5 seems to go with the fifth harmonic of a fundamental frequency $2\pi/16$, when we were expecting a fundamental frequency of $10\pi/16$ for the cosine. In fact, this happens often when we use the DFT because all the frequencies have to be integer multiples of $\hat{\omega}_1 = 2\pi/N$.

This example illustrates the fact that it is impossible to get a consistent relationship between the fundamental period and fundamental frequency of a discrete-time signal. ■

66-7.2 Sampling Bandlimited Periodic Signals

The next task will be to relate the DFS to the continuous-time Fourier Series. The connection is sampling above the Nyquist rate. Consider a periodic bandlimited continuous-time signal represented by the following *finite* Fourier series

$$x(t) = \sum_{m=-M}^{M} a_m e^{j2\pi f_0 m t} \qquad -\infty < t < \infty, \tag{66.78}$$

where f_0 is the fundamental frequency (in Hz) and m denotes the integer index of summation.[11] This continuous-time signal is bandlimited because there is a maximum frequency, $2\pi M f_0$ rad/s, in the expression (66.78) for $x(t)$. When sampling $x(t)$, we must have $f_s > 2Mf_0$ Hz to satisfy the Nyquist rate criterion.

[11] In this chapter, we use the index m for the continuous-time Fourier Series to distinguish it from the discrete-time Fourier Series where we want to use the index k. Previously, in Chapter 3, we used k for the continuous-time Fourier Series summation.

When $x(t)$ is sampled at a rate $f_s = 1/T_s$, the sampled signal $\tilde{x}[n]$ will also be a sum of discrete-time complex exponentials

$$\tilde{x}[n] = x(nT_s) = \sum_{m=-M}^{M} a_m e^{j2\pi f_0 mnT_s} \qquad \text{for } -\infty < n < \infty. \tag{66.79}$$

The discrete-time signal defined in (66.79) might not be periodic, but if $f_s = Nf_0$ then $\tilde{x}[n]$ will be periodic with a period of N. The number of samples in each period (N) will be equal to the duration of the fundamental period (T) times the sampling rate f_s, i.e., $N = f_s/f = (f_s)(T)$ is an integer. We can invert N to write $(1/N) = (1/f_s)(1/T) = (f_0)(T_s)$. When we make the substitution $f_0T_s = 1/N$ in (66.79), the expression for $\tilde{x}[n]$ becomes

$$\tilde{x}[n] = \sum_{m=-M}^{M} a_m e^{j(2\pi/N)mn} \qquad \text{for } -\infty < n < \infty. \tag{66.80}$$

We recognize (66.80) as the *Discrete Fourier Series* of a periodic signal whose period is N. The Fourier Series coefficients are identical for $x(t)$ and $\tilde{x}[n]$.

The number of samples in one period (N) must be large enough so that when we use the DFT of $\tilde{x}[n]$ over one period we will have at least $2M + 1$ DFT coefficients which can be used to get the $2M + 1$ DFS coefficients a_m from $\tilde{X}[k]$ using (66.76). Thus, the DFT-DFS relationship condition requires $N \geq 2M + 1$. In addition, the fact that $f_0T_s = 1/N$ can be rewritten as $f_s = Nf_0$ means that the sampling rate is N times the fundamental frequency of $x(t)$. The Sampling Theorem requirement for no aliasing is $f_s > 2Mf_0$, i.e., the sampling rate must be greater than the Nyquist rate, which is twice the highest frequency in the bandlimited signal $x(t)$. Since $f_s = Nf_0$, the Nyquist rate condition implies that

$$N > 2M \tag{66.81}$$

Therefore, in the $f_s = Nf_0$ case, the number of samples per period must be greater than twice the number of (positive) frequency components in the Fourier representation of $x(t)$.

Example 66-14: Fourier Series of a Sampled Signal

Suppose that the following continuous-time signal

$$x(t) = 2\cos(42\pi t + 0.5\pi) + 4\cos(18\pi t)$$

and we want to determine the Fourier Series representation of the resulting discrete-time signal. In particular, we would like to figure out which Fourier Series coefficients are nonzero. We need a sampling rate that is an integer multiple of the fundamental frequency and is also greater than the Nyquist rate (42 Hz). The two frequency components in $x(t)$ are at 9 Hz and 21 Hz, so the fundamental is $f_0 = 3$ Hz. We must pick $N > 14$ to satisfy the Nyquist rate condition, so for this example we use $f_s = 16 \times 3 = 48$ Hz.

The sum of sinusoids can be converted to a sum of complex exponentials,

$$x(t) = e^{j(42\pi t + 0.5\pi)} + e^{-j(42\pi t + 0.5\pi)} + 2e^{j(18\pi t)} + 2e^{-j(18\pi t)},$$

and then (66.79) can be employed to represent the sampled signal $\tilde{x}[n] = x(n/f_s)$ as

$$\tilde{x}[n] = e^{j(42\pi(n/48) + 0.5\pi)} + e^{-j(42\pi(n/48) + 0.5\pi)} + 2e^{j(18\pi(n/48))} + 2e^{-j(18\pi(n/48))}. \tag{66.82}$$

The four discrete-time frequencies are $\hat{\omega} = \pm(42/48)\pi$ and $\pm(18/48)\pi$. In order to write (66.82) in the summation form of (66.80), we use $N = 16$. In (66.82) we want to emphasize the term $(2\pi/N) = (2\pi/16)$ in the exponents, so we write

$$\tilde{x}[n] = e^{j((2\pi/16)7n+0.5\pi)} + e^{-j((2\pi/16)7n+0.5\pi)} + 2e^{j((2\pi/16)3n)} + 2e^{-j((2\pi/16)3n)}. \tag{66.83}$$

Now we can recognize this sum of four terms as a special case of (66.80) with $N = 16$ and $M = 7$, i.e., the range of the sum is $-7 \leq m \leq 7$. The only nonzero Fourier coefficients in (66.80) are at those for $m = \pm 7, \pm 3$, and their values are $a_3 = 2$, $a_7 = e^{j0.5\pi} = j$, $a_{-3} = 2$, and $a_{-7} = e^{-j0.5\pi} = -j$. ■

These relationships between the DFS (66.80) and the continuous-time Fourier Series (66.78), and also between the DFS and the DFT, are illustrated in Fig. 66-11 where Fig. 66-11(a) shows a "typical" spectrum for a band limited continuous-time periodic signal (as a function of f), and Fig. 66-11(b) shows the spectrum for the corresponding periodic sampled signal (as a function of $\hat{\omega}$ and also k). Notice the alias images of the original spectrum on either side of the *base band* where all the frequencies lie in the interval $-\pi < \hat{\omega}_m \leq \pi$. When $f_s > 2Mf_0$, the sampling rate f_s is greater than the Nyquist rate and the entire continuous-time spectrum is found in the base band because no aliasing distortion occurs.

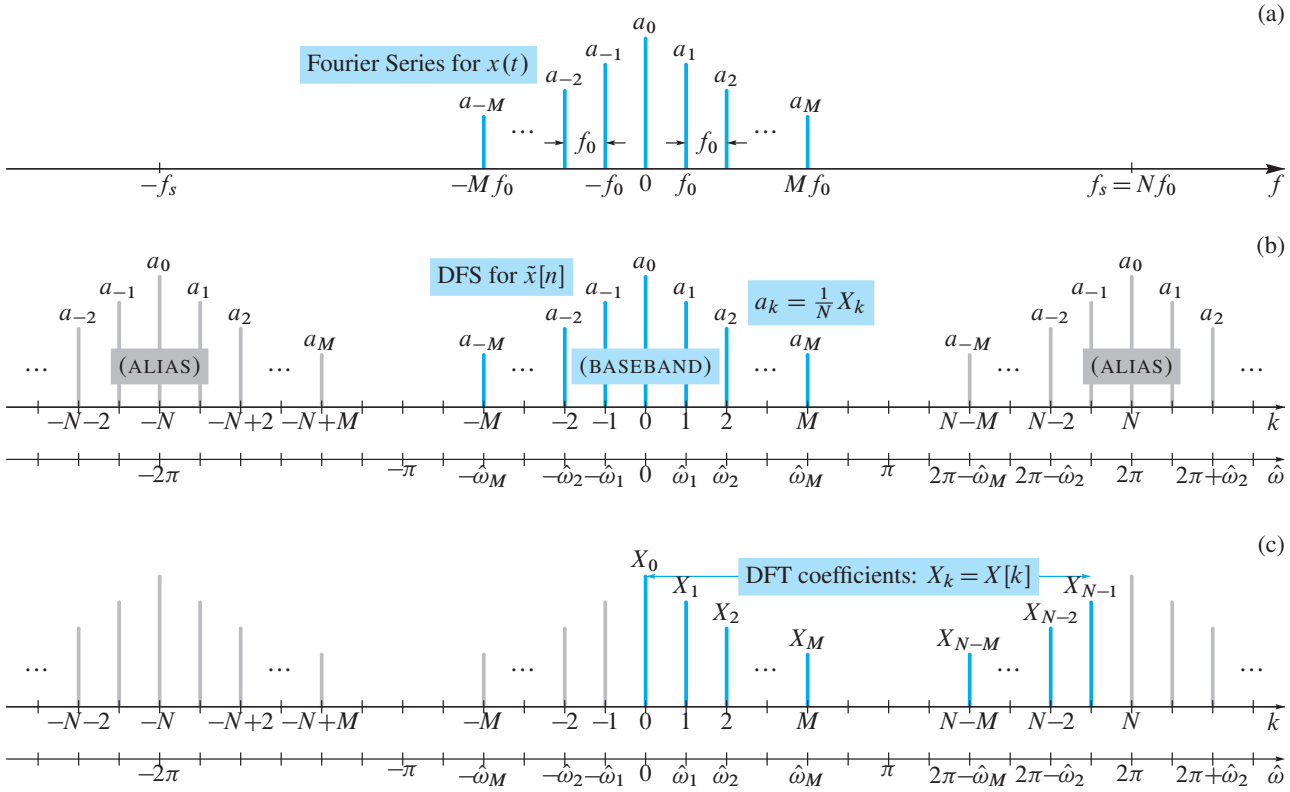

Figure 66-11: Frequency-domain view of sampling a periodic signal. (a) Line spectrum of a bandlimited continuous-time periodic signal whose fundamental frequency is equal to f_0. (b) Line spectrum of the discrete-time periodic signal obtained by sampling the signal in (a) above the Nyquist rate at N times f_0, giving lines at $\hat{\omega}_k = (2\pi/N)k$. (c) DFT coefficients shown as a line spectrum, where the DFT is taken over one period of the periodic discrete-time signal $\tilde{x}[n]$.

We know from Chapter 4 that the spectrum of a sampled signal is periodic in $\hat{\omega}$ with a period of 2π. This attribute is shown in Fig. 66-11(b). Since the spectrum is periodic in $\hat{\omega}$ with a period of 2π with the

spectral lines located at frequencies $\hat{\omega}_k = (2\pi/N)k$, an equivalent statement is that the spectrum is periodic in k with a period equal to N. To emphasize this point, Fig. 66-11(b) shows two horizontal plotting axes: one for normalized frequency $\hat{\omega}$ and the other for the indices k that appear in $\hat{\omega}_k$. The DFT shown in Fig. 66-11(c) is also subject to the same periodicity in k, so the DFT coefficients for $0 \leq k \leq N-1$ can be related to the DFS coefficients via $a_k = (1/N)\tilde{X}[k]$, for $-M \leq k \leq M$.

66-7.3 Spectrum Analysis of Periodic Signals

In this section, we will show how the DFT can be used to analyze continuous-time periodic signals which have been sampled. As a specific example, consider the periodic continuous-time signal

$$\begin{aligned} x_c(t) = {} & 0.1223\cos(2\pi(200)t + 1.5077) \\ & + 0.2942\cos(2\pi(400)t + 1.8769) \\ & + 0.4884\cos(2\pi(500)t - 0.1852) \\ & + 0.1362\cos(2\pi(1600)t - 1.4488) \\ & + 0.0472\cos(2\pi(1700)t) \end{aligned} \tag{66.84}$$

The fundamental frequency of this signal is $\omega_0 = 2\pi(100)$ rad/sec, and the signal consists of five harmonics at 2, 4, 5, 16, and 17 times the fundamental. This signal is the same as the synthetic vowel studied in Section 3-3.1. If we sample $x_c(t)$ at the rate $f_s = 4000$ Hz, we will obtain exactly 40 samples per period since $f_s = 4000\,\text{Hz}$ is an integer multiple of $f_0 = 100\,\text{Hz}$. The sampled discrete-time signal $x[n] = x_c(n/4000)$ is

$$\begin{aligned} x[n] = {} & 0.1223\cos(0.1\pi n + 1.5077) \\ & + 0.2942\cos(0.2\pi n + 1.8769) \\ & + 0.4884\cos(0.25\pi n - 0.1852) \\ & + 0.1362\cos(0.8\pi n - 1.4488) \\ & + 0.0472\cos(0.85\pi n) \end{aligned} \tag{66.85}$$

The plot of $x[n]$ in Fig. 66-12(a) shows that it is periodic with a period of 40, i.e., $x[n] = x[n+40]$. Another way to arrive at the same conclusion is to note that $x[n]$ has frequencies that are all multiples of $\hat{\omega}_0 = 0.05\pi = 2\pi/40$ which is therefore the fundamental frequency. Like the continuous-time case, $x[n]$ in (66.85) has harmonics at multiples of the normalized fundamental frequency numbered 2, 4, 5, 16, and 17.

Now we consider taking the DFT of $x[n]$ with a DFT length equal to the period. First, one length-40 period of $x[n]$ from Fig. 66-12(a) is extracted and used in a 40-point DFT (66.51). The 40 DFT coefficients $X[k]$ obtained are shown as magnitude and phase in Figs. 66-12(b) and (c), respectively. These 40 DFT coefficients represent one period of the sequence $x[n]$ *exactly* through the synthesis formula of the IDFT (66.52). The DFS is also a representation of $x[n]$ as a sum of complex exponentials at the harmonic frequencies, so the DFT coefficients $X[k]$ are related to the DFS coefficients as shown in (66.76).

EXERCISE 66.19: Use the results of Section 66-7.2, Exercise 66.17 to determine a formula for $X[k]$, the 40-pt. DFT of $x[n]$ in (66.85). Use 40 points of $x[n]$ taken over the period $0 \leq n \leq 39$. Verify that some of the

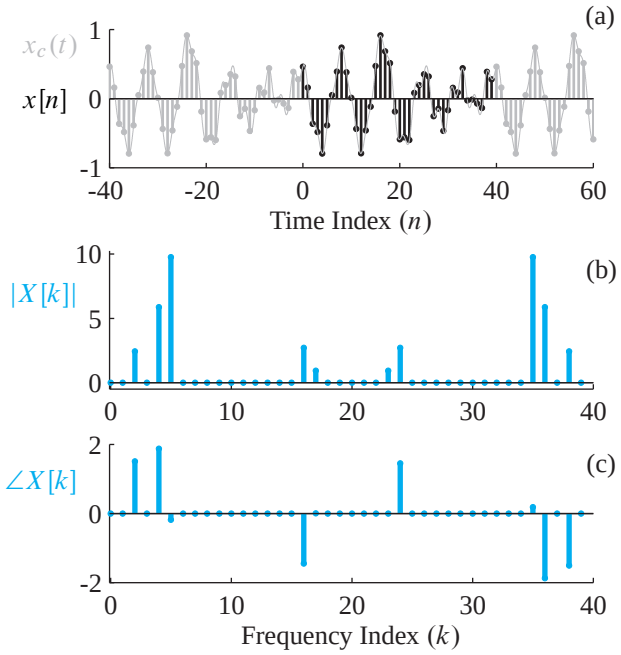

Figure 66-12: Periodic sequence $x[n]$ in (66.85) and the corresponding 40-pt. DFT spectrum $X[k]$. (a) Dark region indicates 40-pt. interval taken for analysis, (b) DFT magnitude spectrum, (c) DFT phase spectrum.

nonzero DFT values are

$$X[k] = \begin{cases} 0.06115(40)e^{j1.5077} & k = 2 \\ 0.1471(40)e^{j1.8769} & k = 4 \\ 0.2442(40)e^{-j0.1852} & k = 5 \\ 0.0681(40)e^{-j1.4488} & k = 16 \\ 0.0236(40) & k = 17 \end{cases} \tag{66.86}$$

Determine the other nonzero values of $X[k]$, and also how many DFT coefficients $X[k]$ are equal to zero.

EXERCISE 66.20: Show that the IDFT of $X[k]$ defined in Exercise 66.19 gives $x[n]$ in (66.85). Furthermore, show that the signal $x[n]$ obtained via the IDFT is periodic with period N.

The plots of Fig. 66-12(b,c) are the spectrum for five sinusoids, or ten complex exponentials, so Fig. 66-12(b) consists of ten spectral lines, each one being just like the plot in Fig. 66-9 which shows the magnitude of the DFT for a single complex exponential signal of the form

$$x[n] = e^{j((2\pi/N)k_0 n + \varphi)} \qquad n = 0, 1, \ldots, N-1$$

where k_0 is an integer.

We have seen that the DFT can be used to obtain the DFS *when the DFT length exactly matches the period of* $x[n]$. Without an exact match, the DFT result might be a reasonable approximation, but it will not be exact. To illustrate this point, consider a case where the sampling frequency is not an integer multiple of the fundamental frequency, i.e., f_s/f_0 is not an integer and, therefore, cannot be equal to the DFT length. An

example is sampling the signal in (66.84) at $f_s = 3950$ Hz, i.e., $f_s/f_0 = 39.5$, so the plot in Fig. 66-13(a) seems to have a period close to 40, but it is not exactly equal to 40.

If we proceed as though the period were 40, and compute the 40-pt DFT of $N = 40$ samples of the sampled signal, we obtain the plot in Fig. 66-13(b). This DFT plot is quite similar to the DFT in Fig. 66-12(b), but none of the DFT coefficients are exactly zero. Instead, each cosine will produce a contribution to the DFT that has many small values spread out over the entire range $0 \le k \le N-1$, as was seen in Fig 66-8. The amplitude of the DFT values will tend to peak around the DFT indices closest to the same peak frequencies as before, $(2\pi f_0/f_s)k$ where $k = 2, 4, 5, 16, 17$. However, the presence of many additional spectral components will give a "blurred" (or imprecise) spectral representation of the original continuous-time signal.

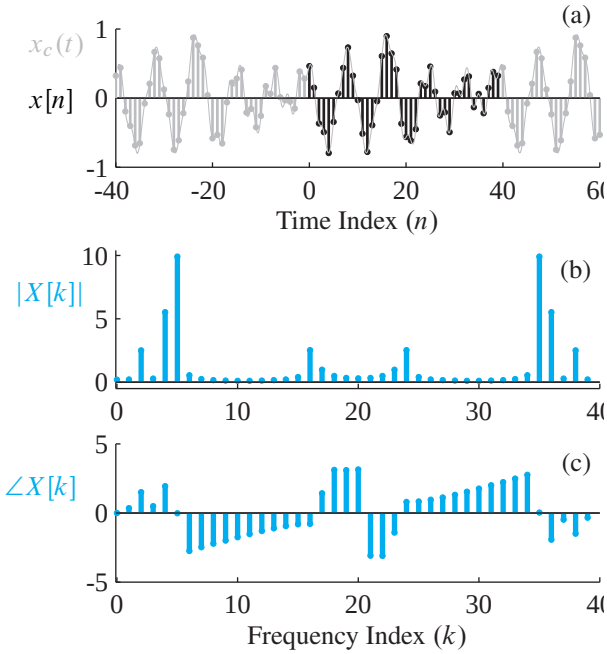

Figure 66-13: Discrete-time sequence $x[n]$ whose period is approximately equal to 40 obtained by sampling $x(t)$ in (66.84) at $f_s = 3950$ Hz, and the corresponding 40-pt. DFT spectrum $X[k]$. (a) Dark region indicates 40-pt. interval taken for analysis, (b) DFT magnitude spectrum, (c) DFT phase spectrum.

EXERCISE 66.21: Use MATLAB to synthesize $N = 40$ samples of $x_c(t)$ in (66.84) with $f_s = 4100$ Hz instead of 4000 Hz; call the result `x4100`. Next, use the MATLAB statement `X41 = fft(x4100,40)` to compute the 40-pt. DFT. Finally, make a plot of the DFT magnitude `stem(0:39,abs(X41))`, and compare the resulting magnitude spectrum to that of Fig. 66-12(b). Comment on zero regions of the DFT.

66-8 Windows

Since the DFT is a finite sum, it can only be used to analyze finite-length signals. Even infinite-length periodic signals that have a DFS are analyzed by taking the DFT of one period. We have examined the case where the finite-length signal is the impulse response of an FIR system, and have shown that samples of the frequency response, or equivalently the DTFT, can be computed by zero-padding and taking a long DFT. Remember from Section 66-6.4 that the N-point DFT of a finite-length sequence is identical to the DTFT of the sequence evaluated at frequencies $\hat{\omega}_k = 2\pi k/N$ with $k = 0, 1, \ldots, N-1$. That is,

$$X[k] = X(e^{j(2\pi k/N)}) = \sum_{n=0}^{L-1} x[n]e^{-j(2\pi k/N)n} \tag{66.87}$$

We recognized that $X[k] = X(e^{j(2\pi k/N)})$ even if $L < N$ since $N-L$ zero samples are effectively appended to the end of the sequence $x[n]$. This operation was called ***zero-padding*** in Section 66-6.4. In MATLAB, the DFT is computed by the function `fft(x,N)`, which automatically zero-pads the sequence if the sequence length is smaller than the DFT length.

In this section, we want to study another aspect of finite-length signals, which is their use as *windows* for local spectrum analysis of short sections of very long signals. The concept of windowing is widely used in signal processing. The basic idea is ***to extract a finite section*** of a very long signal $x[n]$ ***via multiplication*** $w[n]x[n+n_0]$ where n_0 is the starting index of the extracted section. This approach gives a finite-length sequence if the window function $w[n]$ is zero outside of an interval. For example, consider the simplest window function, which is the L-point *rectangular window* defined as

$$w_r[n] = \begin{cases} 1 & 0 \le n \le L-1 \\ 0 & \text{elsewhere} \end{cases} \tag{66.88}$$

The important idea is that the product $w_r[n]x[n+n_0]$ will extract L values from the signal $x[n]$ starting at $n = n_0$. Thus the following are equivalent

$$w_r[n]x[n+n_0] = \begin{cases} 0 & n < 0 \\ \cancel{w_r}^{1}[n]x[n+n_0] & 0 \le n \le L-1 \\ 0 & n \ge L \end{cases} \tag{66.89}$$

The name *window* comes from the idea that we can only "see" the L values of the signal $x[n+n_0]$ within the window interval when we "look" through the window. Multiplying by $w[n]$ is looking through the window. When we change n_0, the signal shifts, and we see a different length-L section of the signal.

The nonzero values of the window function do not have to be all ones, but they should be positive. For example, the symmetric L-point Hann, or von Hann, window[12] is defined as

$$w_h[n] = \begin{cases} 0.5 - 0.5\cos(2\pi(n+1)/(L+1)) & 0 \le n \le L-1 \\ 0 & \text{elsewhere} \end{cases} \tag{66.90}$$

The stem plot of $w_h[n]$ for $L = 20$ in Fig. 66-14 shows that the window values are close to one in the middle and taper off near the ends. In MATLAB the function `hanning(L)` will generate the window values.

[12]The Hann window is named for the Austrian scientist Julius von Hann. This window is often called the "hanning" window. Sometimes, the Hann window formula is given such that $w_h[0] = 0$, but our definition produces all positive values for $w_h[n]$.

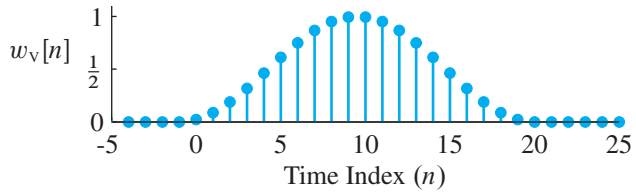

Figure 66-14: Time-domain plot of $L = 20$ Hann window. The window is zero for $n < 0$ and $n \geq 20$.

A related window is the symmetric L-point Hamming window[13] which is defined as

$$w_{hm}[n] = \begin{cases} 0.54 - 0.46\cos(2\pi n/(L-1)) & 0 \leq n \leq L-1 \\ 0 & \text{elsewhere} \end{cases} \tag{66.91}$$

The MATLAB function `hamming(L)` will generate a vector with values given by (66.91).

66-8.0.1 DTFT of Windows

Windows are used often in spectrum analysis because they have desirable properties in the frequency domain. Thus is worth studying the DTFT of a few common windows. We already know the DTFT of the rectangular window—it involves the Dirichlet form.

$$W_r(e^{j\hat{\omega}}) = D_L(\hat{\omega})e^{-j(L-1)\hat{\omega}/2} = \frac{\sin(\frac{1}{2}L\hat{\omega})}{\sin(\frac{1}{2}\hat{\omega})}e^{-j(L-1)\hat{\omega}/2}$$

For the Hamming and von Hann windows, the analytic formulas for the DTFT do not provide much insight, so we prefer to obtain the DTFT numerically and make plots after taking a zero-padded DFT.

Figure 66-15(a) shows plots of the magnitude of the DTFT for two Hann filters with lengths $L = 20$ and $L = 40$. The DTFTs were obtained using a 1024-point DFT with zero padding. The 1024 frequency samples

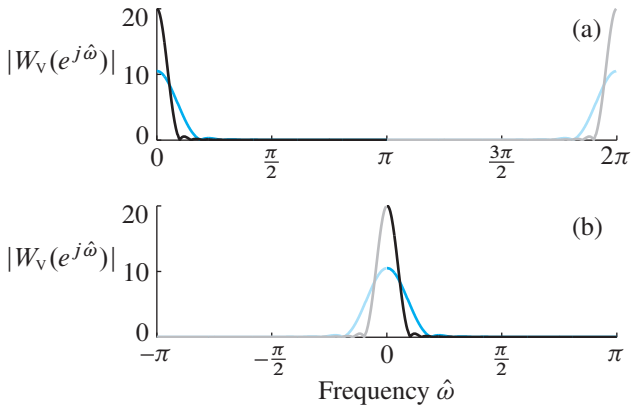

Figure 66-15: DTFT of two Hann windows; length $L = 20$ (colored lines), and length $L = 40$ (black/gray lines) (a) as computed by 1024-point FFT with zero padding and (b) as plotted with DFT values reordered to place $\hat{\omega} = 0$ in the middle.

enable MATLAB's `plot` function to draw a smooth curve even though the sample values are connected by

[13] This window is named for Richard Hamming.

straight lines. Figure 66-15(b) shows that the DTFT of the Hann window is concentrated near $\hat{\omega} = 0$. The main lobe around $\hat{\omega} = 0$ covers the range $-4\pi/(L+1) < \hat{\omega} < 4\pi/(L+1)$; outside of this mainlobe region the DTFT is very close to zero.

When we compare $|W_h(e^{j\hat{\omega}})|$ for the two different window lengths, we see that the DTFT magnitude becomes more concentrated around $\hat{\omega} = 0$ as we increase L. It can be shown that the first zero of $|W_h(e^{j\hat{\omega}})|$ occurs at $\hat{\omega} = 4\pi/(L+1)$ for the Hann filter. Thus, increasing L from 20 to 40 cuts the width of the passband in half (approximately). The peak amplitude at $\hat{\omega} = 0$ is also approximately doubled, going from 10.5 to 20.5, i.e., the general formula for the peak is $\frac{1}{2}(L+1)$. Plotting $|W_h(e^{j\hat{\omega}})|$ allows us to verify these results.

EXERCISE 66.22: There is a property of the DTFT that says the DC value of the DTFT is equal to the sum of all the signal values in the time domain. Use the definition of the forward DTFT to prove this fact.

Windows are used to extract sections of very long signals. An illustrative case is extracting a section of a sinusoid for spectrum analysis, which involves multiplying the sinusoid by the window and taking the DFT with zero padding to obtain samples of the DTFT. Within this context there are two questions that should be answered: first, how to choose a good window, and second, how to choose the window length.

For the first question, consider an example that compares the rectangular window to the Hann window. Suppose that each window is applied to a sinusoid as $x_w[n] = w[n]\cos(0.4\pi n)$, with a window length of 40. Since the window is multiplied by a cosine, the frequency shifting property of the DTFT predicts that the result will be two frequency-shifted copies of the DTFT of the window, i.e.,

$$X_w(e^{j\hat{\omega}}) = \tfrac{1}{2}W(e^{j(\hat{\omega}-0.4\pi)}) + \tfrac{1}{2}W(e^{j(\hat{\omega}+0.4\pi)}) \tag{66.92}$$

where $W(e^{j\hat{\omega}})$ is the DTFT of the window. Figure 66-16 shows the results, and it is easy to see the frequency shifting because the main lobes are centered at $\pm 0.4\pi$. For the rectangular window shown in Fig. 66-16(a),

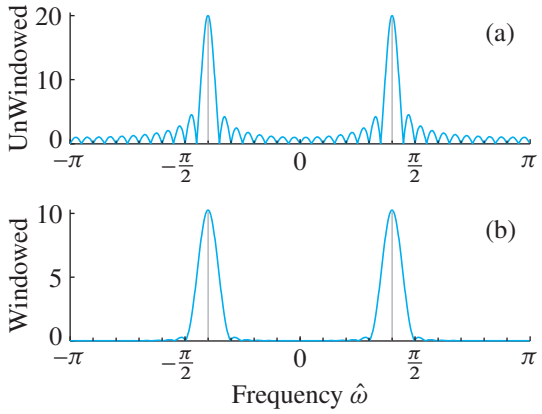

Figure 66-16: DTFT of windowed sinusoid via 1000-pt. DFT for (a) $L = 40$ rectangular window, and (b) $L = 40$ Hann window. Sinusoid frequency is 0.4π rad. Tick marks on frequency axis spaced by 0.1π rad.

the main lobe is narrow, extending over the range $-2\pi/L \leq \hat{\omega} \leq 2\pi/L$ if measured between the first zero crossings on either side of the peak. However, the DTFT magnitude in Fig. 66-16(a) also exhibits many smaller lobes across the entire frequency range. These are called *sidelobes*. For the rectangular window these sidelobes are rather high and are the main reason that this window is considered inferior to most others. On the other hand, the Hann window DTFT shown in Fig. 66-16(b) has a wider mainlobe, but much smaller sidelobes. The

main lobe of the Hann window DTFT extends over the range $-4\pi/L \leq \hat{\omega} \leq 4\pi/L$ when measured between the first zero crossings. Thus the Hann window of length L has a frequency-domain width that is twice that of a rectangular window of the same length. The sidelobes of the Hann DTFT magnitude in Fig. 66-16(b) are less than 1% of the peak heights.

If we pause to ask ourselves what the ideal DTFT should be for a windowed sinusoid, the answer should be that we want to see only two spectrum lines at $\pm\hat{\omega}$. In other words, the ideal main lobe should be very narrow (concentrated at the correct $\pm\hat{\omega}$), and the ideal sidelobes should be zero (or nearly zero). It turns out that these two expectations are in conflict when using finite-length windows, because it can be shown that reducing the sidelobes can only be done at the expense of broadening the main lobe.

Another comparison of the two window DTFTs in Fig. 66-16 shows that the peak heights are different. For the Hann window, we have already observed that the peak height will be $\frac{1}{2}(L+1)$; for the rectangular window it is L. In either case, the window is contributing a known scale factor to the result. If the objective is spectrum analysis of a sinusoid, as in this example, we know that the result should be a spectrum line whose height is half the amplitude of the sinusoid, or $\frac{1}{2}$ in this case. In Fig. 66-16(a) dividing by $L = 40$ will give $\frac{1}{2}$, and also in Fig. 66-16(b) dividing by $\frac{1}{2}(L+1) = 20.5$ will give $\frac{1}{2}$.

For the second question about length of the window, we demonstrated that the width of the mainlobe in the DTFT is inversely proportional to the window length. We continue with the same example of spectrum analysis of a windowed sinusoid, but this time use two different Hann windows with lengths 20 and 40. Figure 66-17 shows the resulting DTFTs. Notice that the known window scale factors have been divided out, so the peak values are $\frac{1}{2}$. If the mainlobe width is measured between first zero crossings, then for Fig. 66-17(a) the

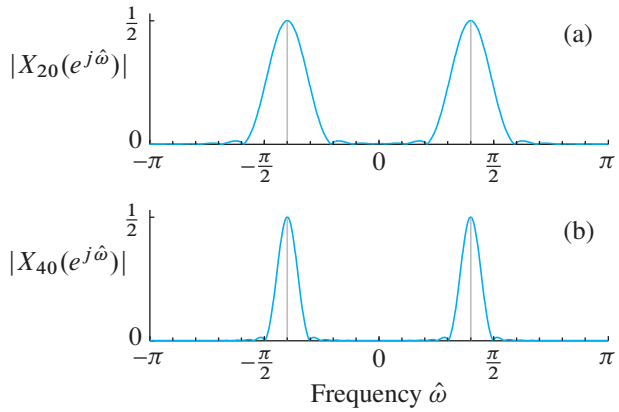

Figure 66-17: DTFT of windowed sinusoid via 1000-pt. DFT for (a) $L = 20$ Hann window, and (b) $L = 40$ Hann window. Sinusoid frequency is 0.4π rad. Tick marks on frequency axis spaced by 0.1π rad.

main lobe extends from 0.2π to 0.6π, and in Fig. 66-17(b) from 0.3π to 0.5π. Thus for $L = 20$, the mainlobe width $\Delta\hat{\omega}$ is $\Delta\hat{\omega} \approx 0.4\pi$, and for $L = 40$, $\Delta\hat{\omega} \approx 0.2\pi$. The dependence of $\Delta\hat{\omega}$ on L is an inverse relationship which can be approximated[14] as $\Delta\hat{\omega} \approx 8\pi/L$.

[14] A precise analysis would show that the first zero crossings are at $\pm 4\pi/(L+1)$, so the exact relationship is $8\pi/(L+1)$. For $L > 30$, the difference in the two formulas is less than 0.1%, and it is easier to remember *inversely proportional to L*.

66-9 The Spectrogram

We have seen that the DFT can *compute* exact frequency-domain representations of both periodic and finite-length discrete-time signals. An equally important case is when the sampled signal is indefinitely long, but not necessarily periodic. Then there are two different viewpoints to consider: the long signal has the same *global* spectral content for its entire duration, or the long signal is actually the concatenation of many short signals with changing *local* spectral content. In the first case, we might be able to analyze the signal mathematically with the DTFT, but we cannot *numerically calculate* its frequency domain representation unless the long signal is actually a finite-length signal. Then we could compute its DFT but we we might have to wait an inordinately long time just to acquire all the samples, and even having done so, we would then be faced with a huge DFT computation. This would be unacceptable in a real-time system that needs to process signals on-line. When the long signal is the concatenation of many short signals, the appropriate frequency-domain representation would be the collection of many short-length DFTs. Then the temporal variations of the *local* frequency content would stand out. The spectrogram arises from this viewpoint where a short-length DFT is used to repeatedly analyze different short sections of a longer signal.

Good examples of indefinitely long signals are audio signals such as speech or music. In both of these cases, it is the temporal variation of the frequency content that is of interest. The pitch and timbre of speech which changes with time is how information is encoded in human speech. Likewise, we have already seen that music can be synthesized as a succession of tone combinations held constant for short time intervals. For audio signals we may have digital recordings that give a very long sequence obtained by sampling for many minutes or even hours. For example, one hour of stereophonic music sampled at 44.1 kHz would be represented by $44100 \times 60 \times 60 = 158{,}760{,}000$ samples per channel. If we want to compute the (global) DFT of the entire one hour of audio, the closest power-of-two FFT needed would be $N = 2^{28} = 268{,}435{,}456$ per channel. On the other hand, the local spectrum approach above would use short-length FFTs to analyze short time segments within the long signal. This is reasonable (and generally preferable) because a long recording probably contains a succession of short passages where the spectral content does not vary. In addition, there may be a natural segment length for the audio signal that will dictate the FFT length.

66-9.1 An Illustrative Example

To examine the points made above, we shall study a signal whose spectral properties vary with time. We begin by synthesizing a continuous-time signal that consists of four contiguous time intervals of cosine waves of different amplitudes and constant frequencies. Such a signal could be described by the equation

$$x(t) = \begin{cases} 5\cos(2\pi f_0 t) & 0 \le t < T_1 \\ 2\cos(2\pi f_1 t) & T_1 \le t < T_2 \\ 2\cos(2\pi f_2 t) & T_2 \le t < T_3 \\ 0.5\cos(2\pi f_3 t) & T_3 \le t < T_4 \\ \quad \cdots & T_4 \le t \end{cases} \tag{66.93}$$

The signal $x(t)$ begins with a T_1-second interval of a cosine signal of amplitude 5 and frequency f_0 Hz. At $t = T_1$ the waveform switches to a cosine of amplitude 2 and frequency f_1, and retains these parameters throughout the interval $T_1 \le t < T_2$. The last two intervals switch to different amplitude and frequency parameters at T_2 and T_3 as described by (66.93). The signal might continue indefinitely with changing parameters after $t = T_4$, but it is sufficient to limit attention to the first four time intervals.

For a particular sampling frequency f_s, the resulting sampled signal would be

$$x[m] = x(m/f_s) = \begin{cases} 5\cos(\hat{\omega}_0 m) & 0 \le m \le 499 \\ 2\cos(\hat{\omega}_1 m) & 500 \le m \le 2999 \\ 2\cos(\hat{\omega}_2 m) & 3000 \le m \le 4999 \\ 0.5\cos(\hat{\omega}_3 m) & 5000 \le m \le 9999 \end{cases} \tag{66.94}$$

where $\hat{\omega}_0 = 2\pi f_0/f_s$, $\hat{\omega}_1 = 2\pi f_1/f_s$, $\hat{\omega}_2 = 2\pi f_2/f_s$ and $\hat{\omega}_3 = 2\pi f_3/f_s$ are dimensionless frequency quantities, and the durations are $T_1 f_s = 500$, $T_2 f_s = 3000$, $T_3 f_s = 5000$, and $T_4 f_s = 10000$ samples. Figure 66-19(a) shows the first 801 samples of $x[m]$ when $\hat{\omega}_0 = 0.211\pi$, $\hat{\omega}_1 = 0.111\pi$, $\hat{\omega}_2 = 0.8\pi$, and $\hat{\omega}_3 = 0.4\pi$. These normalized frequencies would be the result when $f_s = 2000$ Hz and $f_0 = 211$ Hz, $f_1 = 111$, and $f_2 = 800$, and $f_3 = 400$ Hz. However, other values of f_0, f_1, f_2, f_3, and f_s could give the same normalized frequencies and, therefore, the same sequence of samples.

EXERCISE 66.23: Suppose that the sampling frequency is $f_s = 1000$ Hz. What values of f_0, f_1 f_2, and f_3 in (66.93) will give values $\hat{\omega}_0 = 0.211\pi$, $\hat{\omega}_1 = 0.111\pi$, $\hat{\omega}_2 = 0.8\pi$, and $\hat{\omega}_3 = 0.4\pi$ in (66.94)?

EXERCISE 66.24: Create the sampled signal $x[m]$ in (66.94) with frequencies $\hat{\omega}_0 = 0.211\pi$, $\hat{\omega}_1 = 0.111\pi$, $\hat{\omega}_2 = 0.8\pi$, and $\hat{\omega}_3 = 0.4\pi$, and then use the D-to-A converter on your computer (`soundsc` in MATLAB) with $f_s = 2000$ Hz to listen to $x(t)$ in (66.93). During the listening observe the differences among the four segments of the signal. Is what you hear completely consistent with the specified signal parameters (duration, frequency, intensity) given above for (66.93)?

Now suppose that we compute the DFT of the entire 10000-point sequence $x[m]$ in (66.94) using zero padding with $N = 16384$. The resulting magnitude of the length-16384 DFT is plotted in Fig. 66-18. The

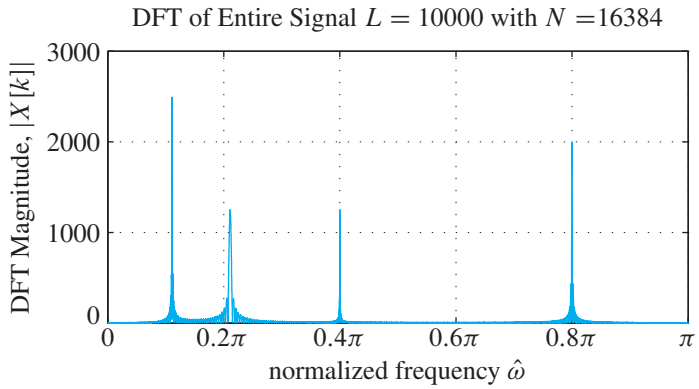

Figure 66-18: DFT of the entire sequence $x[n]$ in (66.94) with DFT length $N = 16384$. Only the magnitude $|X[k]|$ is shown for $0 \le k \le 8192$. Horizontal axis is labeled with normalized frequency using $\hat{\omega}_k = 2\pi k/N$.

obvious features in this figure are four narrow peaks and these give some clues as to the nature of the signal $x[n]$, but the interpretation is far from complete and is not straightforward. The four strong peaks might suggest a signal comprised of a sum of four cosine waves of different frequencies and comparable amplitudes. With some assurance, we can state the following about the signal whose DFT is plotted in Fig. 66-18:

1. The four peaks in the DFT spectrum occur at frequencies corresponding to approximately $\hat{\omega} = 0.111\pi$, 0.211π, 0.4π, and 0.8π, so they probably represent sine or cosine wave components in $x[n]$ at those frequencies.

2. The peak heights of the DFT are not an unambiguous indicator of the amplitudes of the sinusoidal components because, as demonstrated in Section 66-6.6, the peak height of the DFT of a cosine signal depends on both the amplitude of the cosine signal and its duration. The peak heights in Fig. 66-18 differ at most by a factor of two, but we know in this example that the actual amplitudes for frequencies 0.111π, 0.211π, 0.4π, and 0.8π are 2, 5, 0.5, and 2, respectively. Although the height of the 0.211π peak is equal to the height of the peak at 0.4π, in fact, there is a 10:1 ratio between the amplitudes of those cosine components. Similarly, the DFT peak heights at 0.211π and 0.111π are in the ratio 1:2, while we know that the ratio of amplitudes of those two cosines is 5:2. The reason for this is that the DFT of a cosine of amplitude A and duration L achieves a maximum of approximately $AL/2$, as was demonstrated in Section 66-6.6. The amplitude and duration of the $\hat{\omega}_0 = 0.211\pi$ segment are $A_0 = 5$ and $L_0 = 500$, while the corresponding values for the $\hat{\omega}_3 = 0.4\pi$ segment are $A_3 = 0.5$ and $L_3 = 5000$; therefore, the peak heights are the same: $5 \times 500/2 = 0.5 \times 5000/2 = 1250$.

3. Figure 66-18 tells us nothing about the time location or time variation of the signal properties. For example, we cannot tell whether the different components occur simultaneously (overlapping in time through the whole analysis interval) or sequentially (as they do in this example). This is because in either case, the signals are additively combined, and by the linearity of the DFT, the result is the sum of all the DFTs of the individual components.
   Aside: The change in starting time is a time shift of a signal which does change the phase, but not the magnitude of the DFT.

66-9.2 Time-Dependent DFT

Thus, we see that the long DFT gives useful information about the frequency content of a signal such as $x[n]$ in (66.94), but it would be much more useful if the DFT could be used also to track the time-varying properties of the signal. To formalize this concept for a signal $x[m]$ that is an indefinitely long sequence, we define the *time-dependent discrete Fourier transform* of this signal as

$$X[k,n] = \sum_{m=0}^{L-1} w[m]x[n+m]e^{-j(2\pi k/N)m} \qquad k = 0, 1, \ldots, N-1 \tag{66.95}$$

where n is the ***analysis time index*** that specifies where in $x[n]$ a short-length DFT will be taken. This equation involves two steps: windowing and short-length DFTs. First of all, $w[m]$ is called the ***analysis window***. It is a sequence such as the Hann window in (66.90) that is nonzero only in the interval $m = 0, 1, \ldots, L-1$, where L is assumed to be much smaller than the total length of the sequence $x[m]$. Therefore, the product $w[m]x[n+m]$ is also nonzero only for $m = 0, 1, \ldots, L-1$. In this way, the window *selects* a finite-length segment from the sequence $x[m]$ in the neighborhood of the analysis time index n. Second, a short-length DFT of the finite-length windowed segment is computed to extract the spectrum for that local interval of the signal. By adjusting the analysis time index n, we can move any desired segment of $x[m]$ into the domain of the window, and thereby select L samples for analysis. The length-L segments are often called *frames*. Because the window imposes time localization, $X[k,n]$ in (66.95) is also known as the ***short-time discrete Fourier transform*** or ***STDFT***.

Now the right-hand side of (66.95) is easily recognized as the N-point DFT of the finite-length sequence $w[m]x[n+m]$, so (66.95) can be evaluated efficiently for each choice of n by an FFT computation. The

selection of analysis segments is illustrated by Fig. 66-19 for two values of the the analysis time index n, $n = 0$ and $n = 400$. Figure 66-19(a) shows the first 801 samples of the discrete-time signal $x[m]$ in (66.94) plotted versus m with dots for signal values. Also shown in Fig. 66-19(a) are two shaded regions of length 301 samples. One region starts at $n = 0$ and is shaded in color, and the other starts at $n = 400$ and is shaded in gray.[15] These are potential 301-sample analysis frames. Also shown in Fig. 66-19(a) is the outline of the (bell-shaped) Hann window $w[m]$ whose origin is fixed at $m = 0$.[16] The colored samples in Fig. 66-19(a) are the samples that are

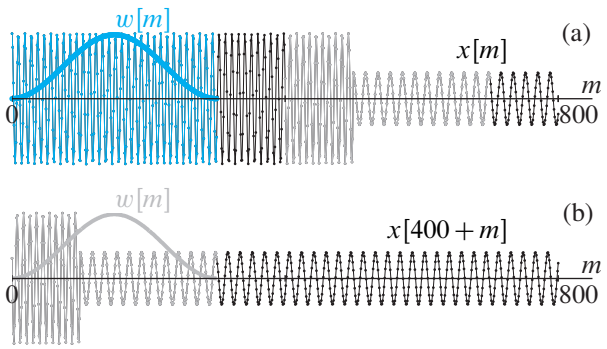

Figure 66-19: Time-dependent Hann windowing of a signal using a length-301 window. (a) The signal $x[m+0] = x[m]$ and fixed window $w[m]$, (b) Fixed window $w[m]$ with signal shifted by 400 samples, i.e., $x[m+400]$.

multiplied by the window $w[m]$ when $n = 0$ and are thus selected for analysis with the DFT to obtain $X[k, 0]$, the DFT of $w[m]x[m+0]$.

Figure 66-19(b) shows the fixed window sequence (in gray) along with the sequence $x[m+400]$, i.e., the sequence $x[m]$ shifted to the left by 400 samples. The gray samples in Figs. 66-19(a) and (b) are the same; in Fig. 66-19(b) these samples are multiplied by the window and are thus selected for DFT analysis to compute $X[k, 400]$. To compute $X[k, n]$ for any other value of n, we simply form the "windowed" sequence $w[m]x[m+n]$ in the manner illustrated in Fig. 66-19 and then compute the DFT of the resulting finite-length sequence as in (66.95). The shift n is typically moved in jumps of R samples, where $1 \leq R < L$. A common default choice is $R = L/2$, but the choice of R can affect the smoothness of tracking the temporal changes in a signal. As long as $R < L$ the windowed segments will overlap and all samples of the signal will be included in at least one analysis window.

To illustrate the nature of the short-time DFT, Fig. 66-20 shows plots of $|X[k, 250]|$, $|X[k, 2000]|$, $|X[k, 4000]|$, and $|X[k, 6000]|$ for the signal of (66.94) with STDFT parameters $L = 301$ and $N = 1024$. Figure 66-20 confirms that $|X[k, 250]|$, $|X[k, 2000]|$, $|X[k, 4000]|$, and $|X[k, 6000]|$ each display a single peak centered at the frequency of the sinusoidal component at the corresponding *analysis* times. Furthermore, the amplitudes of the peaks are in correct proportion since for the analysis times chosen, there is only one frequency within the window and the window lengths are the same ($L = 301$).[17]

While plots like those in Fig. 66-20 are useful for displaying the frequency-domain properties in the neighborhood of a specific analysis time n, they do not give a complete overview of how the signal parameters vary with time. In this example, we selected the analysis time indices $n = 250, 2000, 4000$, and 6000, because we knew that these positions would show the different frequencies. In a practical setting, where we do not know the details of the signal in advance, the spectrogram display is much more effective and widely used.

[15] The shading of the samples is intended to emphasize two typical analysis intervals, with the implication that in general, all the samples would be plotted with the same color.

[16] The discrete-time window sequences are shown as continuous functions to distinguish them from the samples of $x[m]$.

[17] The absolute height of the peaks depends on the window; specifically, $\sum w[m]$.

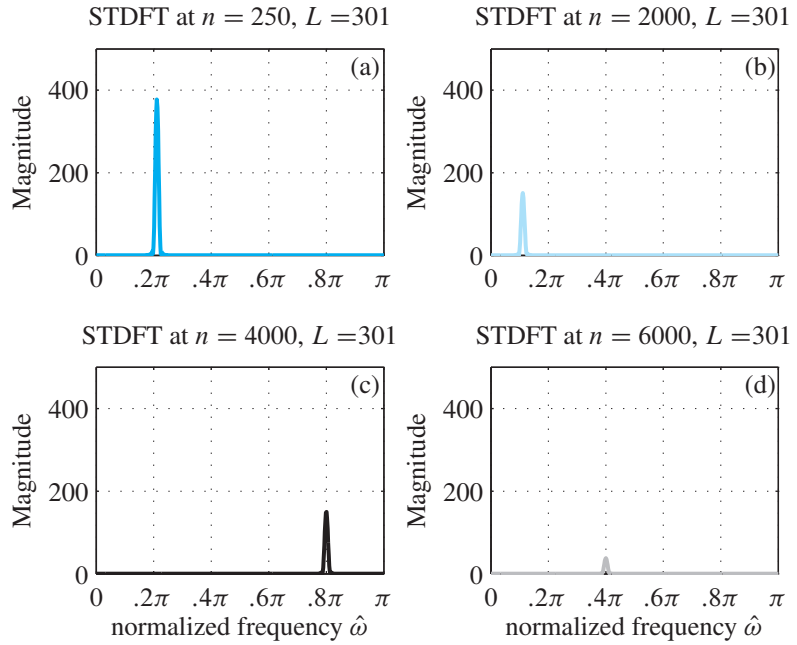

Figure 66-20: Short-time spectra for signal in Fig. 66-19 with $L = 301$ and $N = 1024$. (a) STDFT at analysis time index $n = 250$. (b) STDFT at $n = 2000$. (c) STDFT at $n = 4000$. (d) STDFT at $n = 6000$. *Note:* DFT magnitudes for $0 \leq k \leq 512$ are connected as if plotting the corresponding DTFT at frequencies $0 \leq \hat{\omega} \leq \pi$.

66-9.3 The Spectrogram Display

The STDFT computation results in a two-dimensional function $X[k,n]$, where the k dimension represents frequency because $\hat{\omega}_k = (2\pi k/N)$ is the k^{th} analysis frequency, and the n dimension represents time since the analysis window-position times are $t_n = nT_s$. Since the STDFT is a function of both frequency and time, there might be a different *local spectrum* for each analysis time. Although $X[k,n]$ is complex valued with a magnitude and phase, we usually plot only the magnitude versus (k,n) with a three-dimensional graphical display. A variety of display methods can be used to plot the magnitude $|X[k,n]|$ as a function of both k and n, including waterfall plots (a sequence of plots like those in Fig. 66-20 stacked vertically), perspective plots, contour plots, or grayscale images. In addition, plotting the log magnitude, $\log|X[k,n]|$ versus (k,n), is often used to show a wider amplitude range. The preferred form is the ***spectrogram***, which is a grayscale (or pseudocolor) image where the gray level at point (k,n) is proportional to the magnitude $|X[k,n]|$ or the log magnitude, $\log|X[k,n]|$. Usually, large magnitudes are rendered as black, and small ones white, but pseudocolor images are also common.

Spectrograms of the signal in (66.94) are shown in Fig. 66-21; other examples can be seen in Figs. 13-18, 13-20, 13-22, 13-23, 13-25, and 13-27. The horizontal axis is analysis time and the vertical axis is frequency. Analysis time can be given as a sample index (n) as in Fig. 66-21, or converted to continuous-time $t_n = n/f_s$ via the sampling rate. Likewise, frequency can be converted from the index k to hertz, or to normalized frequency $\hat{\omega}$ as in Fig. 66-21. In the spectrogram image for a real signal, usually only the frequency range for $0 \leq k \leq N/2$, or $0 \leq \hat{\omega} \leq \pi$ is shown because the negative frequency region is conjugate symmetric. For the complex signal case, the frequency range is either $0 \leq \hat{\omega} < 2\pi$, or $-\pi < \hat{\omega} \leq \pi$, depending on whether or not the FFT values are reordered prior to being displayed.[18]

[18] The *SP-First* toolbox functions `plotspec` and `spectgr`, which are similar to MATLAB's function `spectrogram`, use the ordering

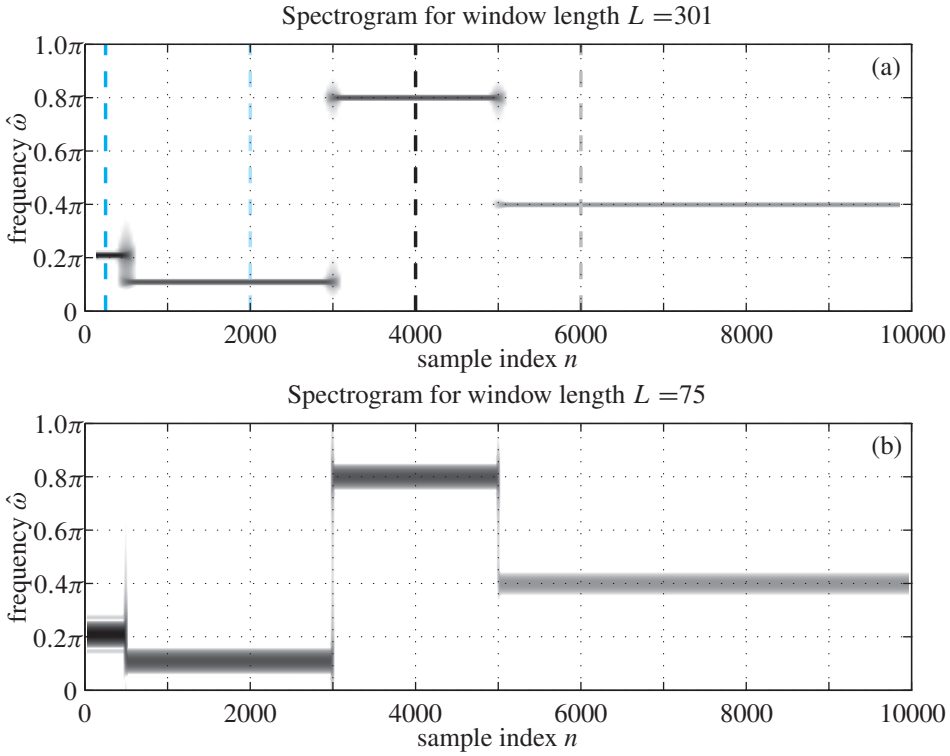

Figure 66-21: Spectrograms of test signal calculated with `spectgr` (linear magnitude). (a) Window length $L = 301$. (b) Window length $L = 75$. For both cases, $N = 1024$ and $R \approx 0.1L$.

66-9.4 Interpretation of the Spectrogram

A glance at Fig. 66-21 confirms that the spectrogram provides a much clearer time-frequency picture of the characteristics of the signal defined in (66.94) than does either the single plot of a long DFT as in Fig 66-18, or the four snapshots in Fig. 66-20. The four sinusoidal components and their starting/ending times are evident in Fig. 66-21(a). On the other hand, the dark horizontal bars in Fig. 66-21(b) are wider and less clearly defined, so it is hard to determine the exact frequency. However, it is clear in both spectrograms where the sinusoidal components are located in time. The dashed lines at $n = 250$, $n = 2000$, $n = 4000$ and $n = 6000$ show the locations of four individual DFTs that comprise Fig. 66-20. That is, the DFT plots in Figs. 66-20(a), (b), (c) and (d) are columns of the gray-scale spectrogram image shown in Fig. 66-21(a). The magnitude of the DFT is mapped to a gray-scale shading which is visible along the colored, black and gray vertical marker lines, respectively. Figures 66-20(a–d) are, therefore, "vertical slices" of the spectrogram.

A comparison of the two spectrograms in Fig. 66-21 yields some valuable insight into the effect of the window length in short-time Fourier analysis. The window length is $L = 301$ in Fig. 66-21(a) and $L = 75$ in Fig. 66-21(b). Along the time axis (n) at points where the frequency changes abruptly, there are "blurry" regions; these occur at $n = 500, 3000$, and 5000. The blurred regions occur whenever the analysis window straddles a region of rapid change since we will have signal samples within the window from both sides of the change point. For example, when $n = 350$, the signal interval $[350, 650]$ will be shifted under the $L = 301$ point window prior to the DFT, so the first half of $x[350 + m]$ will have frequency 0.211π and the second half will have frequency 0.111π. Thus the STDFT $X[k, 350]$ should have lower peaks at both frequencies. The

$-\pi < \hat{\omega} \leq \pi$ for complex signals; MATLAB's `spectrogram` function uses $0 \leq \hat{\omega} < 2\pi$.

longer the window, the wider will be this fuzzy region of ambiguity. This effect is seen in a comparison of Figs. 66-21(a) and (b) because the regions of fuzziness are much wider for the $L = 301$ window. This example illustrates the general principle that *precise location of temporal changes in the signal requires a short window*.

66-9.4.1 Frequency Resolution

Another important point is that the vertical width of the horizontal bars (for the sinusoids) is different in the two spectrograms. In fact, the width of the bars in Fig. 66-21(b) is approximately 4 times the width of the bars in Fig. 66-21(a), while the window lengths are 75 and 301, respectively. This suggests that for a signal having multiple frequency components overlapping in time, the spectrogram may not show two distinct peaks if the frequencies are too close together. In other words, the spectrogram may need a longer window to "resolve" two closely spaced frequency components into separate peaks in the frequency domain.

This ***resolution*** issue is illustrated by a test example where the signal is composed of multi-frequency sinusoids with closely spaced frequencies. The two spectrograms shown in Fig. 66-22 were computed for two different window lengths for the signal

$$x[m] = \begin{cases} \cos(0.2\pi m) + 1.5\cos(0.227\pi m) & 0 \le m < 5000 \\ \cos(0.2\pi m) & 5000 \le m < 7000 \\ 3\cos(0.6\pi m) + \cos(0.7\pi m) & 7000 \le m < 10000, \end{cases} \tag{66.96}$$

By comparing the spectrograms we can see the effect of the window length on frequency resolution. During the

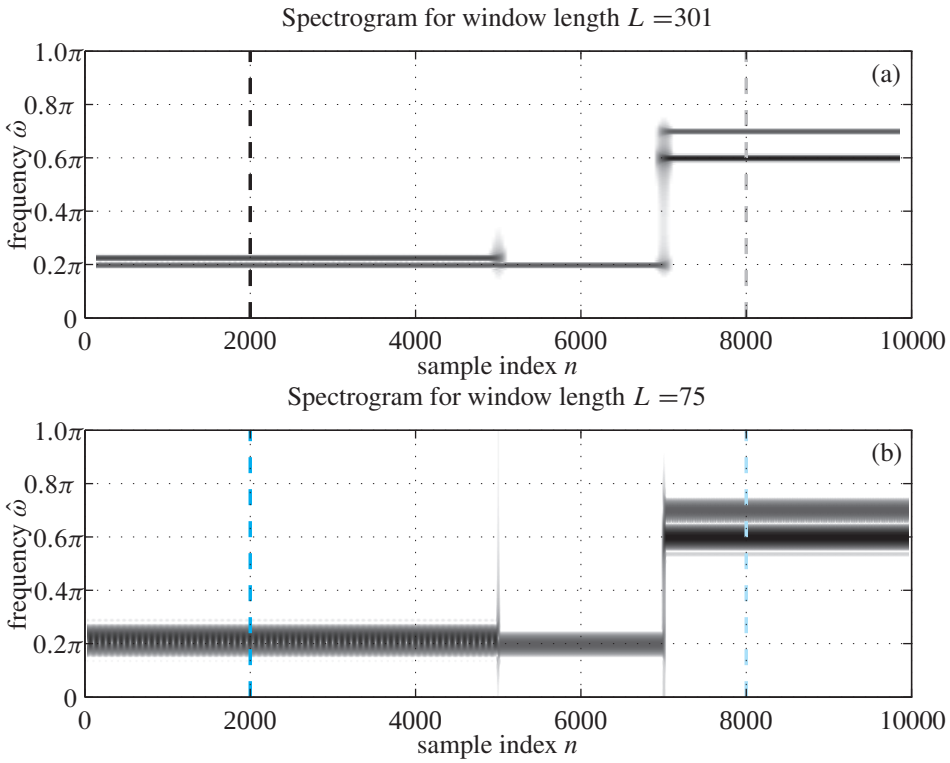

Figure 66-22: Spectrograms of test signal. (a) Window length $L = 301$. (b) Window length $L = 75$. FFT length was 1024 with zero padding.

first interval the two frequencies are very close together at 0.2π and 0.227π (a spacing of 0.027π rad), while

in the third interval, the two frequencies are farther apart at 0.6π and 0.7π (a spacing of 0.1π rad). The two frequencies in the first interval are both evident in Fig. 66-22(a), but not in Fig. 66-22(b) where they are merged into a single broad horizontal bar. On the other hand, during the third time interval, two clearly separated bars are evident in both spectrograms at the frequencies 0.6π and 0.7π, i.e., the two frequency components are *resolved*. This resolution is possible because, although the bars in Fig. 66-22(b) are 3–4 times wider than the corresponding features in Fig. 66-22(a), the spacing between the frequencies 0.7π and 0.6π is approximately four times the spacing between 0.227π and 0.2π. This example illustrates the general principle that *frequency resolution can be improved by lengthening the analysis window*.

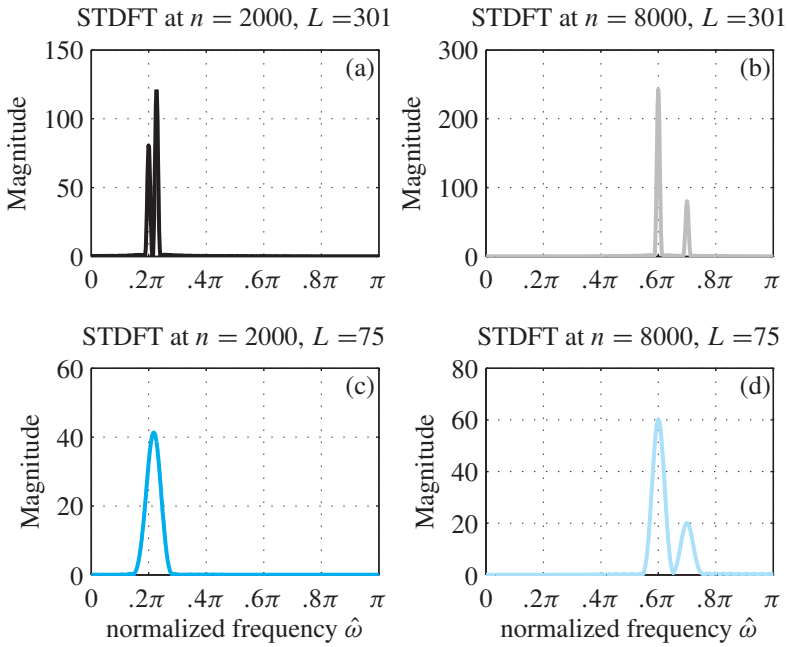

Figure 66-23: Short-time spectra for signal in (66.94) at two different time indices. (a) Hann window length $L = 301$, time index $n = 2000$. (b) $L = 301$, $n = 8000$, (c) $L = 75$, $n = 2000$, and (d) $L = 75$, $n = 8000$. FFT length was 1024 with zero padding.

To see the frequency resolution more clearly, Fig. 66-23 shows "vertical slices" taken along the dashed lines in Fig. 66-21(a) and (b) corresponding to analysis times $n = 2000$ and 8000, which are in the middle of the segments having two sinusoids with closely spaced frequencies. Figure 66-23(a) corresponds to the slice at $n = 2000$ with the window length $L = 301$, and it shows two distinct peaks around the frequencies 0.2π and 0.227π. However, Fig. 66-23(c) shows the slice at $n = 2000$ with the window length $L = 75$. In this case there is only a single broad peak, and we conclude that the two frequencies are "not resolved." On the other hand, for the slices at $n = 8000$ shown in Figs. 66-23(b) and (d), the two frequencies are more widely separated, and we see two distinct peaks in both of the spectrogram slices. However, for the slice at $n = 8000$, if the window length were reduced below 75, the two peaks in Fig. 66-23(d) would broaden and eventually as the window length decreases we would see only a single broad peak spanning the two frequencies at 0.6π and 0.7π. As a final comment, note that the vertical slice DFTs show clearly that the amplitude of the two sinusoids is different, but the amplitude difference is much harder to discern in the gray-scale spectrogram image.

EXERCISE 66.25: Use MATLAB to generate the signal

$$x[m] = 3\cos(0.6\pi m) + \cos(0.7\pi m) \quad 7000 \le m < 10000$$

Then using a Hann window, compute the spectrogram slice at $n = 8000$. Use window lengths of $L = 61$ and $L = 31$ and compute the DFTs to produce plots like Fig. 66-23(b). Determine whether or not the two sinusoidal components are "resolved."

As suggested by Fig. 66-23, the width of the peaks for the DFTs of the sinusoidal components depends inversely on the window length L. In the previous section 66-8, we learned that what we are seeing in Fig. 66-23(a) is the DTFT of the window $w[n]$ shifted in frequency to the frequency of the sinusoid. Furthermore, it is a general principle of Fourier transforms that there is an inverse relation between window length and frequency width. Therefore, the frequency width of the DTFT of a window sequence such as the Hann window can be written as an inverse relationship

$$\Delta\hat{\omega} \approx \frac{C}{L}$$

where the constant C is a small number, usually $4\pi < C < 8\pi$ for "good" windows. For the Hann window, the zero-crossing width is $\Delta\hat{\omega} = 8\pi/L$, so $\Delta\hat{\omega} = 8\pi/75 = 0.107\pi$ for the length-75 Hann window, which is enough to resolve the 0.6π and 0.7π frequency peaks at $n = 8000$. If two frequencies differ by less than $\Delta\hat{\omega}$, their STDFT peaks will blend together. Thus, the ability to resolve two sinusoids, i.e., see two distinct peaks, depends inversely on the window length L. This makes sense intuitively because the longer the window, the longer the time to observe the periodicity (or non-periodicity) of a signal. On the other hand, if the window is very short, e.g., less than one period of the signal, then we have virtually no information about any periodicity of the signal, and it is reasonable to expect this to be reflected in the STDFT.

There is still one more point to make about the window length, and this is the issue of "time resolution." We observed in Fig. 66-21 that the window length is also important in tracking the temporal changes in a signal. The "fuzzy" transition regions are approximately 4 times as wide in Fig. 66-21(a) as in Fig. 66-21(b) because the window length goes from $L = 301$ to $L = 75$. Therefore, a rule of thumb often given is that in order to track rapid changes, we need to keep the window length as short as possible.

We are forced, therefore, into a tradeoff situation: the window should be short to track temporal changes, but long to resolve closely-spaced frequency components. For this reason, when studying the properties of an unknown signal, it is common to compute spectrograms with differing window lengths. Features that are obvious in one case may be obscured in another, but with multiple spectrograms and a good understanding of how window length (and shape) affect the spectrogram image, it is often possible to determine much useful information about the signal. This time-frequency information can be combined with physical models for signal generation and/or detection to obtain very accurate models of the signal that can be useful in a variety of applications. A notable and ubiquitous application is audio coding for digital storage and transmission. Audio coders like MP3 are based upon the same type of frequency analysis computations employed to generate the spectrogram image. Because the human auditory system incorporates a type of frequency analysis, short-time frequency-domain analysis is a very natural way to incorporate auditory perception effects such as masking into the process of compressing the digital representation of an audio signal. By a careful frequency analysis "frame by frame", it is possible to mask coding errors by literally "hiding" them beneath prominent spectral components.

66-9.5 Spectrograms in MATLAB

Since the spectrogram can be computed by doing many FFTs of windowed signal segments, MATLAB is an ideal environment for doing the DFT calculation and displaying the image. Specifically, the MATLAB spectrogram computation evaluates (66.95) for length-L signal segments that are separated by R, i.e., $n = 0, R, 2R, 3R, \ldots$.

$$X[(2\pi k/N)f_s, rRT_s] = \sum_{m=0}^{L-1} w[m]x[rR+m]e^{-j(2\pi k/N)m} \qquad k = 0, 1, \ldots, N/2 \tag{66.97}$$

Quite often the default is $R = L/2$, so there is a 50% overlap of the signal segments analyzed by the DFT after windowing. The value of N is the DFT length, so zero padding would be done when $N > L$. Picking a large value for N will give many frequency samples along the k dimension because the frequency index k ranges from 0 to $N/2$. When the sampling rate $f_s = 1/T_s$ associated with $x[n]$ is available, the frequency locations for the DFT output can be scaled to hertz and the time axis can be converted from sample index to analysis time in seconds which is convenient for labeling the axes of the spectrogram display.[19]

The computation of the spectrogram can be expressed in a simple MATLAB program that involves one `for` loop. The core of the program is shown below for the special case of an even-length window with 50% overlap of signal segments.

```
% L = signal segment length, also window length (even integer)
% N = FFT (DFT) lengths
% wn = window signal, L-point column vector such as the Hann window, or hanning.m
% xn = input signal (column vector)
% assume the overlap is 50%
Lx = length(xn);
NwinPos = 2*ceil(Lx/L);
X = zeros(N,NwinPos);
for ii=0:NwinPos-1
   X(:,ii) = fft(wn.*xn(ii*L/2 + (1:L)),N);
end
```

In recent versions of MATLAB the command that invokes the computation of (66.97) is

```
[S,F,T] = spectrogram(X,WINDOW,NOVERLAP,NFFT,Fs,'yaxis')
```

The final string `'yaxis'` is needed to override the default behavior that puts the frequency axis on the horizontal and the time axis vertical. The outputs from `spectrogram` are `S`, a two-dimensional array containing the *complex-valued* spectrogram values, `F`, a vector of all the analysis frequencies, and `T`, a vector containing the starting times of the signal segments being windowed. The inputs are the signal `X`, the window coefficients `WINDOW`, the overlap of signal segments `NOVERLAP`, the FFT length `NFFT`, and the sampling frequency `Fs`. In addition, the default `spectrogram` window is Hamming, so it should be replaced with a call to the Hann function, e.g., `hanning(L)`. Note that the window skip parameter R in (66.97) is the window length minus the overlap, so the overlap should be less than the window length, but choosing `Noverlap` equal to `length(window)-1`

[19] In other words, MATLAB's spectrogram function calibrates the frequency and time axes in continuous-time units assuming a given sampling rate f_s.

would generate a lot of needless computation (and possibly a very large image!), because the window skip would be $R = 1$. It is common to pick the overlap to be somewhere between 50 percent and 90 percent of the window length i.e., $0.1L \leq R \leq 0.5L$, depending on how smooth the final spectrogram image needs to be. See `help spectrogram` in MATLAB for more details.

The spectrogram image can be displayed by using any one of MATLAB's 3-D display functions. To get the inverted gray-scale images shown in this chapter, use the following:

```
imagesc( T, F, abs(S) )
axis  xy, colormap(1-gray)
```

The color map of `(1-gray)` gives a negative gray scale that is useful for printing, but on a computer screen it might preferable to use color, e.g., `colormap(jet)`. Finally, it may be advantageous to use a logarithmic amplitude scale in `imagesc` in order to see tiny amplitude components, as well as big ones.

66-10 The Fast Fourier Transform (FFT)

The material in this section is optional reading. It is included for completeness, since the FFT is the most important algorithm and computer program for doing spectrum analysis.

66-10.1 Derivation of the FFT

In Section 66-5.2 we discussed the FFT as an efficient algorithm for computing the DFT. In this section, we will give the basic divide-and-conquer method that leads to the FFT. From this derivation, it should be possible to write an FFT program that runs in time proportional to $(N/2)\log_2 N$ time. We need to assume that N is a power of two, so that the decomposition can be carried out recursively. Such algorithms are called *radix-2* algorithms.

The DFT summation (**??**) and the IDFT summation (**??**) are essentially the same, except for a minus sign in the exponent of the DFT and a factor of $1/N$ in the inverse DFT. Therefore, we will concentrate on the DFT calculation, knowing that a program written for the DFT could be modified to do the IDFT by changing the sign of the complex exponentials and multiplying the final values by $1/N$. The DFT summation can be broken into two sets, one sum over the even-indexed points of $x[n]$ and another sum over the odd-indexed points.

$$X[k] = \text{DFT}_N\{x[n]\} \tag{66.98}$$

$$= \sum_{n=0}^{N-1} x[n]e^{-j(2\pi/N)kn} \tag{66.99}$$

$$= \left(x[0]e^{-j0} + x[2]e^{-j(2\pi/N)2k} + x[N-2]e^{-j(2\pi/N)k(N-2)}\right) + \left(x[1]e^{-j(2\pi/N)k} + x[3]e^{-j(2\pi/N)3k} + x[N-1]e^{-j(2\pi/N)k(N-1)}\right) \tag{66.100}$$

$$X[k] = \sum_{\ell=0}^{N/2-1} x[2\ell]e^{-j(2\pi/N)k(2\ell)} + \sum_{\ell=0}^{N/2-1} x[2\ell+1]e^{-j(2\pi/N)k(2\ell+1)} \tag{66.101}$$

At this point, two clever steps are needed: First, the exponent in the second sum must be broken into the product of two exponents, so we can factor out the one that does not depend on ℓ. Second, the factor of two in the exponents (2ℓ) can be associated with the N in the denominator of $2\pi/N$.

$$\begin{aligned} X[k] &= \sum_{\ell=0}^{N/2-1} x[2\ell]e^{-j(2\pi k/N)(2\ell)} \\ &\quad + e^{-j(2\pi k/N)} \sum_{\ell=0}^{N/2-1} x[2\ell+1]e^{-j(2\pi k/N)(2\ell)} \\ X[k] &= \sum_{\ell=0}^{N/2-1} x[2\ell]e^{-j(2\pi k/(N/2))\ell} \\ &\quad + e^{-j(2\pi k/N)} \sum_{\ell=0}^{N/2-1} x[2\ell+1]e^{-j(2\pi k/(N/2))\ell} \end{aligned}$$

Now we have the correct form. Each of the summations is a DFT of length $N/2$, so we can write

$$\begin{aligned} X[k] &= \mathrm{DFT}_{N/2}\{x[2\ell]\} \\ &\quad + e^{-j(2\pi/N)k}\ \mathrm{DFT}_{N/2}\{x[2\ell+1]\} \end{aligned} \tag{66.102}$$

The formula (66.102) for reconstructing $X[k]$ from the two smaller DFTs has one hidden feature: It must be evaluated for $k = 0, 1, 2, \ldots, N-1$. The $N/2$-point DFTs give output vectors that contain $N/2$ elements; e.g., the DFT of the odd-indexed points would be

$$X^o_{N/2}[k] = \mathrm{DFT}_{N/2}\{x[2\ell+1]\}$$

for $k = 0, 1, 2, \ldots, N/2-1$. Thus we need an extra bit of information to calculate $X[k]$, for $k \geq N/2$. It is easy to verify that

$$X^o_{N/2}[k + N/2] = X^o_{N/2}[k]$$

and likewise for the DFT of the even-indexed points, so we need merely to periodically extend the results of the $N/2$-point DFTs before doing the sum in (66.102). This requires no additional computation.

The decomposition in (66.102) is enough to specify the entire FFT algorithm: Compute two smaller DFTs and then multiply the outputs of the DFT over the odd indices by the exponential factor $e^{-j(2\pi/N)k}$. Refer to Fig. 66-24, where three levels of the recursive decomposition can be seen. If a recursive structure is adopted, the two $N/2$ DFTs can be decomposed into four $N/4$-point DFTs, and those into eight $N/8$-point DFTs, etc. If N is a power of two, this decomposition will continue ($\log_2 N - 1$) times and then eventually reach the point where the DFT lengths are equal to two. For two-point DFTs, the computation is trivial:

$$\begin{aligned} X_2[0] &= x_2[0] + x_2[1] \\ X_2[1] &= x_2[0] + e^{-j2\pi/2}\, x_2[1] = x_2[0] - x_2[1] \end{aligned}$$

The two outputs of the two-point DFT are the sum and the difference of the inputs. The last stage of computation would require $N/2$ two-point DFTs.

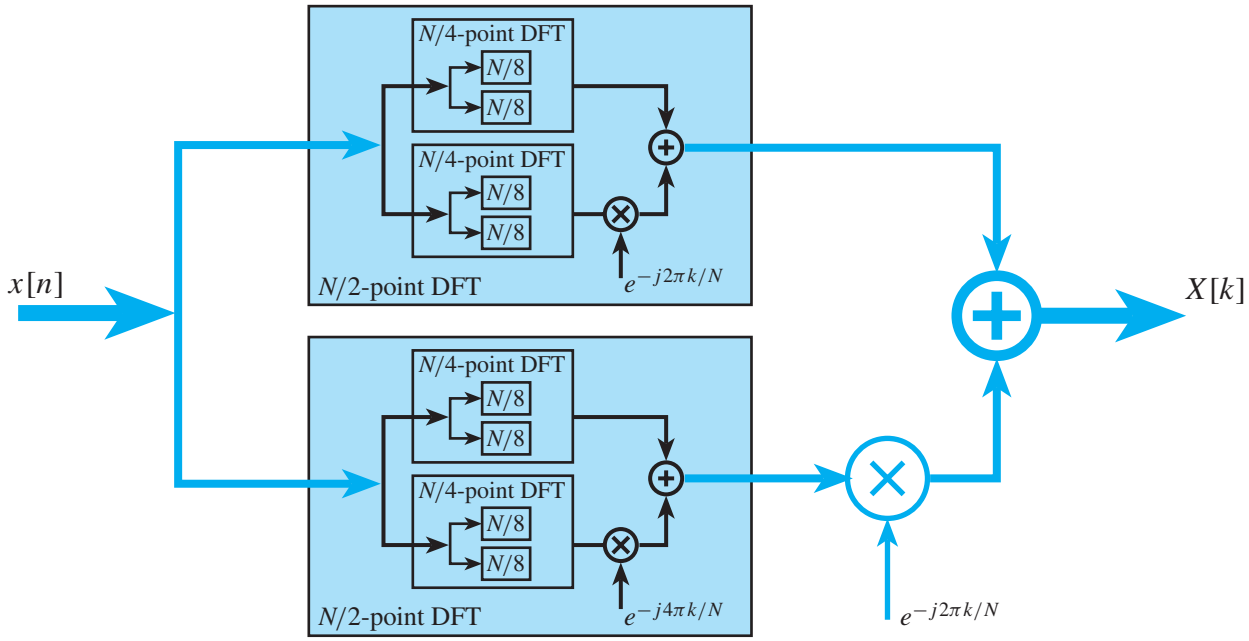

Figure 66-24: Block diagram of a radix-2 FFT algorithm for $N = 2^{\nu}$. The width of the lines is proportional to the amount of data being processed. For example, each $N/4$-point DFT must transform a data vector containing $N/4$ elements. (Chapter13/art/FFTdecompFixed)

66-10.1.1 FFT Operation Count

The foregoing derivation is a bit sketchy, but the basic idea for writing an FFT program using the two-point DFT and the complex exponential as basic operators has been covered. However, the important point about the FFT is not how to write the program, but rather the number of operations needed to complete the calculation. When it was first published, the FFT made a huge impact on how people thought about problems, because it made the frequency-domain accessible numerically. Spectrum analysis became a routine calculation, even for very long signals. Operations such as filtering, which seem to be natural for the time-domain, could be done more efficiently in the frequency-domain for very long FIR filters.

The number of operations needed to compute the FFT can be expressed in a simple formula. We have said enough about the structure of the algorithm to count the number of operations. The count goes as follows: the N point DFT can be done with two $N/2$ point DFTs followed by N complex multiplications and N complex additions, as we can see in (66.102).[20] Thus, we have

$$\mu_c(N) = 2\mu_c(N/2) + N$$
$$\alpha_c(N) = 2\alpha_c(N/2) + N$$

where $\mu_c(N)$ is the number of complex multiplications for a length-N DFT, and $\alpha_c(N)$ is the number of complex additions. This equation can be evaluated successively for $N = 2, 4, 8, \ldots$, because we know that $\mu_c(2) = 0$ and $\alpha_c(2) = 2$. Table 66-3 lists the number of operations for some transform lengths that are powers of two. The formula for each can be derived by matching the table:

[20] Actually, the number of complex multiplications can be reduced to $N/2$, because $e^{-j2\pi(N/2)/N} = -1$.

Table 66-3: Number of operations for radix-2 FFT when N is a power of two. Notice how much smaller $\mu_c(N)$ is than $4N^2$.

N	$\mu_c(N)$	$\alpha_c(N)$	$\mu_r(N)$	$\alpha_r(N)$	$4N^2$
2	0	2	0	4	16
4	4	8	16	16	64
8	16	24	64	48	256
16	48	64	192	128	1024
32	128	160	512	320	4096
64	320	384	1280	768	16384
128	768	896	3072	1792	65536
256	1792	2048	7168	4096	262144
⋮	⋮	⋮	⋮	⋮	⋮

$$\mu_c(N) = N(\log_2 N - 1)$$
$$\alpha_c(N) = N \log_2 N$$

Since complex number operations ultimately must be done as multiplies and adds between real numbers, it is useful to convert the number of operations to real adds and real multiplies. Each complex addition requires two real additions, but each complex multiplication is equivalent to four real multiplies and two real adds. Therefore, we can put two more columns in Table 66-3 with these counts.

The bottom line for operation counts is that the total count is something proportional to $N \log_2 N$. The exact formulas from Table 66-3 are

$$\mu_r(N) = 4N(\log_2 N - 1)$$
$$\alpha_r(N) = 2N(\log_2 N - 1) + 2N = 2N \log_2 N$$

for the number of real multiplications and additions, respectively. Even these counts are a bit high because certain symmetries in the complex exponentials can be exploited to further reduce the computations.

66-11 Summary and Links

In this chapter we introduced the discrete Fourier transform (DFT) and discrete-time Fourier transform (DTFT), and we have shown how these concepts can be useful in computing spectrum representations of signals and for understanding the behavior of linear systems. We showed how the DFT can be derived from the Fourier series integral for continuous-time periodic signals, and we showed how the DFT could be used in a variety of ways. We also showed the relationship between the DFT and the DTFT and illustrated how the DTFT can simplify the solution of problems involving linear time-invariant systems. In subsequent chapters, we will see how the DFT and DTFT are related to yet another transform called the z-transform.